First results on the experimental search for η' mesic nuclei with the $^{12}C(p,d)$ reaction

Yoshiki K. Tanaka (GSI)

for η-PRiME/Super-FRS collaboration

Y. Ayyad, J. Benlliure, K.-T. Brinkmann, S. Friedrich, H. Fujioka, H. Geissel, J. Gellanki, C. Guo, E. Gutz, E. Haettner, M. N. Harakeh, R. S. Hayano, Y. Higashi, S. Hirenzaki, C. Hornung, Y. Igarashi, N. Ikeno, K. Itahashi, M. Iwasaki, D. Jido, N. Kalantar-Nayestanaki, R. Kanungo, R. Knöbel, N. Kurz, V. Metag, I. Mukha, T. Nagae, H. Nagahiro, M. Nanova, T. Nishi, H. J. Ong, S. Pietri, A. Prochazka, C. Rappold, M. P. Reiter, J.L. Rodríguez-Sánchez C. Scheidenberger, H. Simon, B. Sitar, P. Strmen, B. Sun, K. Suzuki, I. Szarka, M. Takechi, Y. K. Tanaka, I. Tanihata, S. Terashima, Y. N. Watanabe, H. Weick, E. Widmann, J. S. Winfield, X. Xu, H. Yamakami, J. Zhao

RCNP Osaka University, Universidade de Santiago de Compostela, Universität Giessen, Kyoto University, GSI, KVI-CART University of Groningen, Beihang University, The University of Tokyo, Nara Women's University, KEK, Tottori University, RIKEN Nishina Center, Tokyo Metropolitan University, Saint Mary's University, Comenius University Bratislava, Stefan Meyer Institut, Niigata University

GSI

η' PRiME

η′ meson bound states in nuclei

η′ meson in vacuum

η'

- Mass = 958 MeV/c^2 (especially large), Width : 0.2 MeV, $J^P = 0^-$
- $U_A(1)$ anomaly and spontaneous breaking of chiral symmetry

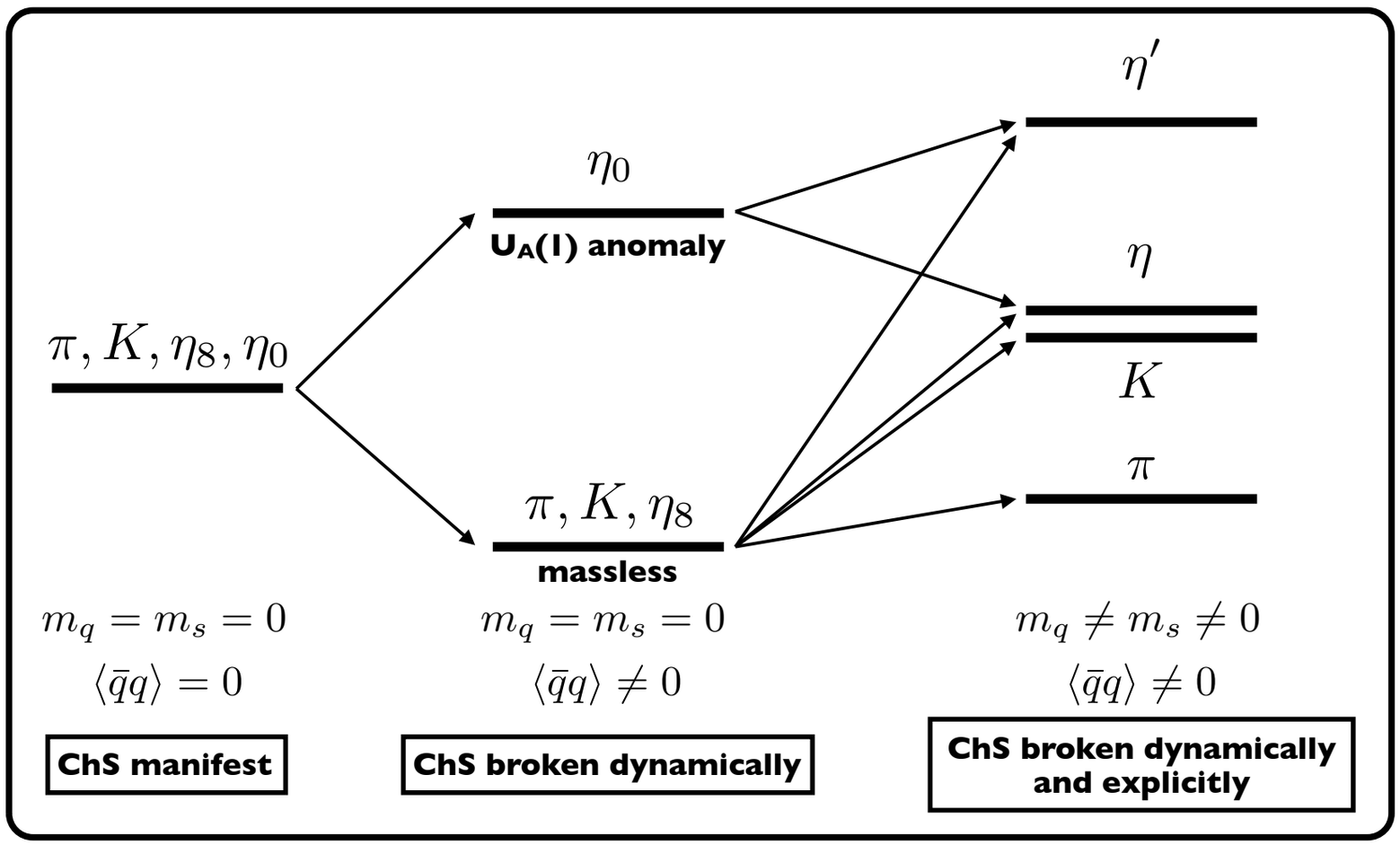

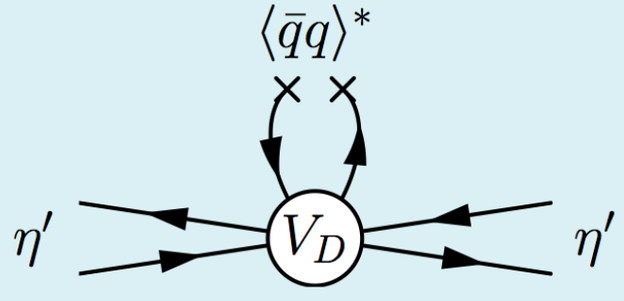

$U_A(1)$ anomaly contributes η' mass through ChSB

H. Nagahiro *et al*,
PRC 87, 045201 (2013).

D. Jido, H. Nagahiro, S. Hirenzaki,
PRC 85, 032201 (2012).

η′ meson bound states in nuclei

η′ meson in vacuum

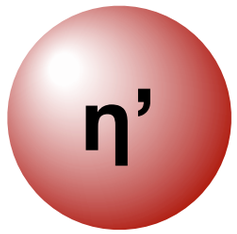

- Mass = 958 MeV/c^2 (especially large), Width : 0.2 MeV, $J^P = 0^-$
- $U_A(1)$ anomaly and spontaneous breaking of chiral symmetry

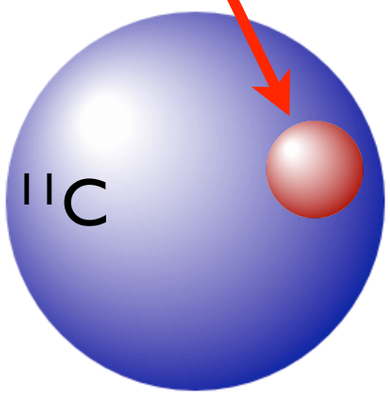

η′ meson at nuclear density

- Partial restoration of chiral symmetry ($\langle \bar{q}q \rangle$ reduced ~ 30%)
- Mass reduction is expected

η′ meson bound states in nuclei

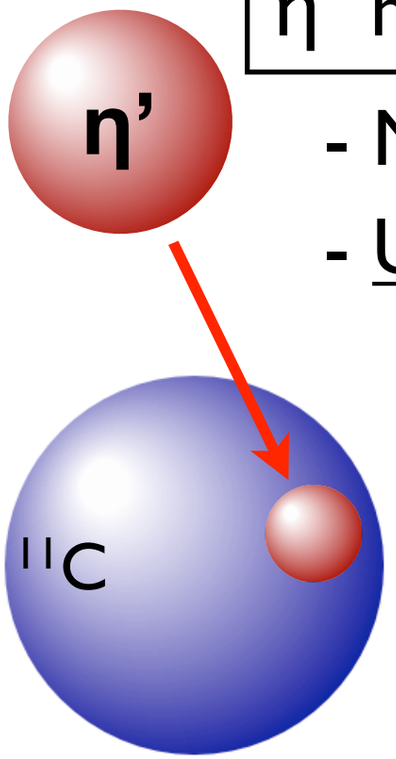

η′ meson in vacuum

- Mass = 958 MeV/c^2 (especially large), Width : 0.2 MeV, $J^P = 0^-$
- $U_A(1)$ anomaly and spontaneous breaking of chiral symmetry

η′ meson at nuclear density

- Partial restoration of chiral symmetry ($\langle \bar{q}q \rangle$ reduced ~ 30%)
- Mass reduction is expected

NJL model

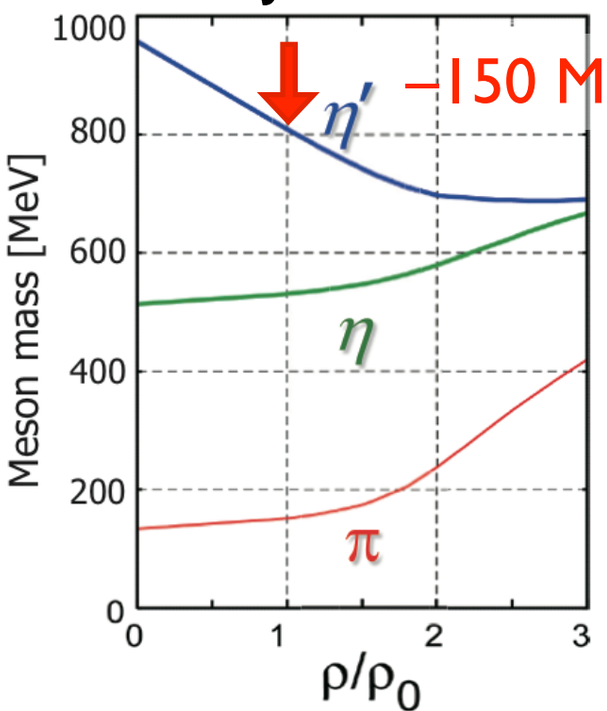

linear σ model

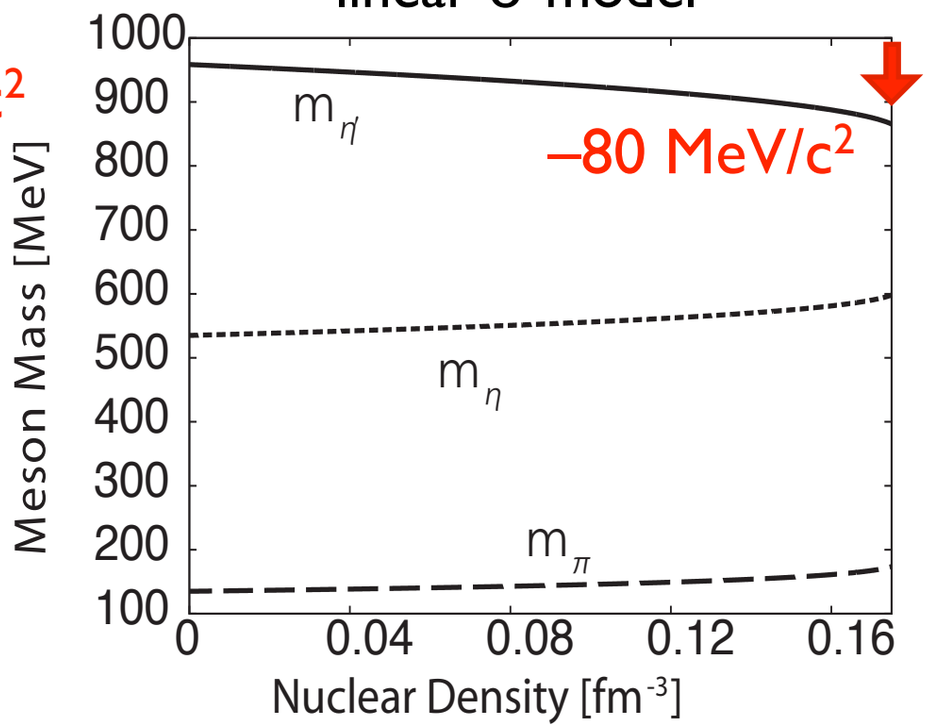

QMC model :
$\Delta m \sim -37$ MeV/c^2
(for $\theta_{\eta\eta'} = -20°$)

H. Nagahiro *et al.*, PRC 74, 045203(2006).
S. Sakai *et al.*, D. Jido, PRC 88, 064906 (2013).
S.D. Bass, A.W. Thomas, PLB 634, 368 (2006).

η′ meson bound states in nuclei

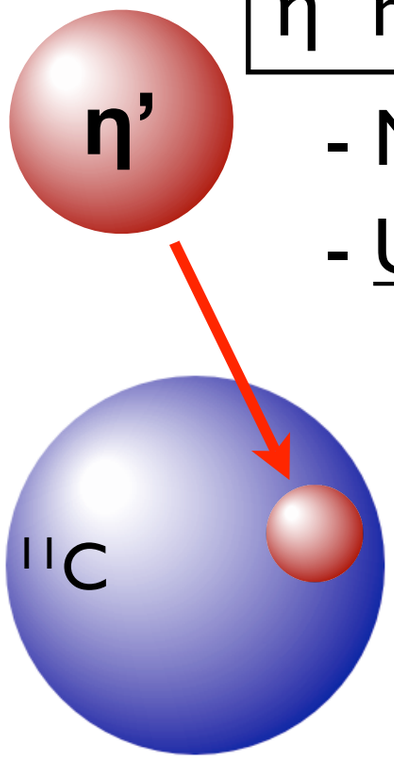

η′ meson in vacuum

- Mass = 958 MeV/c^2 (especially large), Width : 0.2 MeV, $J^P = 0^-$
- $U_A(1)$ anomaly and spontaneous breaking of chiral symmetry

η′ meson at nuclear density

- Partial restoration of chiral symmetry ($\langle \bar{q}q \rangle$ reduced ~ 30%)
- Mass reduction is expected

⬇

η′ nucleus optical potential: $V_{\eta'} = (V_0 + iW_0)\frac{\rho(r)}{\rho_0}$

$V_0 = \Delta m(\rho_0)$, $W_0 = -\Gamma(\rho_0)/2$

⬇

η′ meson nucleus bound states (η′ mesic nuclei)
→ direct probe for in-medium meson properties

η′-nucleus potential

η′-nucleus optical potential : $V_{\eta'} = (V_0 + iW_0)\frac{\rho(r)}{\rho_0}$

$V_0 = \Delta m(\rho_0)$, $W_0 = -\Gamma(\rho_0)/2$

Theoretical predictions

$\Delta m(\rho_0) \sim -150$ MeV (NJL model)

H. Nagahiro *et al.*, PRC 74, 045203(2006).
P. Costa *et al.*, PRD 71, 116002 (2005).

~ -80 MeV (linear σ model)

S. Sakai, D. Jido, PRC 88, 064906 (2013)

~ -37 MeV (QMC model) for $\theta_{\eta\eta'}$=−20°

S.D. Bass, A.W. Thomas, PLB 634, 368 (2006)

η′-nucleus potential

η′-nucleus optical potential : $V_{\eta'} = (V_0 + iW_0)\frac{\rho(r)}{\rho_0}$

$V_0 = \Delta m(\rho_0)$, $W_0 = -\Gamma(\rho_0)/2$

Theoretical predictions

$\Delta m(\rho_0) \sim -150$ MeV (NJL model)

H. Nagahiro *et al.*, PRC 74, 045203(2006).
P. Costa *et al.*, PRD 71, 116002 (2005).

~ -80 MeV (linear σ model)

S. Sakai, D. Jido, PRC 88, 064906 (2013)

~ -37 MeV (QMC model) for $\theta_{\eta\eta'} = -20°$

S.D. Bass, A.W. Thomas, PLB 634, 368 (2006)

Experimental indications by CBELSA/TAPS

- $V_0 = -39 \pm 7(\text{stat}) \pm 15(\text{syst})$ MeV
- $W_0 = -13 \pm 3(\text{stat}) \pm 3(\text{syst})$ MeV

M. Nanova *et al.*, PRC 94 025205 (2016).
M. Nanova *et al.*, PLB 727, 417 (2013).
M. Nanova *et al.*, PLB 710, 600 (2012).
S. Friedrich *et al.*,EPJA 52, 297 (2016).

η′-nucleus potential

η′-nucleus optical potential : $V_{\eta'} = (V_0 + iW_0)\frac{\rho(r)}{\rho_0}$

$V_0 = \Delta m(\rho_0)$, $W_0 = -\Gamma(\rho_0)/2$

Theoretical predictions

$\Delta m(\rho_0) \sim -150$ MeV (NJL model)

H. Nagahiro *et al.*, PRC 74, 045203(2006).
P. Costa *et al.*, PRD 71, 116002 (2005).

~ -80 MeV (linear σ model)

S. Sakai, D. Jido, PRC 88, 064906 (2013)

~ -37 MeV (QMC model) for $\theta_{\eta\eta'} = -20°$

S.D. Bass, A.W. Thomas, PLB 634, 368 (2006)

Experimental indications by CBELSA/TAPS

- $V_0 = -39 \pm 7(\text{stat}) \pm 15(\text{syst})$ MeV
- $W_0 = -13 \pm 3(\text{stat}) \pm 3(\text{syst})$ MeV

M. Nanova *et al.*, PRC 94 025205 (2016).
M. Nanova *et al.*, PLB 727, 417 (2013).
M. Nanova *et al.*, PLB 710, 600 (2012).
S. Friedrich *et al.*,EPJA 52, 297 (2016).

η′-*p* scattering length by COSY-11

E. Czerwiński et al., PRL 113, 062004 (2014)

- $\mathrm{Re}(a_{\eta' p}) = 0 \pm 0.43$ fm, $\mathrm{Im}(a_{\eta' p}) = 0.37^{+0.40}_{-0.16}$ fm

→ $|V_0| < 38$ MeV, $W_0 = -(33^{+40}_{-14})$ MeV (low density approx.)

η′-nucleus potential

η′-nucleus optical potential :

$$V_{\eta'} = (V_0 + iW_0)\frac{\rho(r)}{\rho_0}$$

$V_0 = \Delta m(\rho_0)$, $W_0 = -\Gamma(\rho_0)/2$

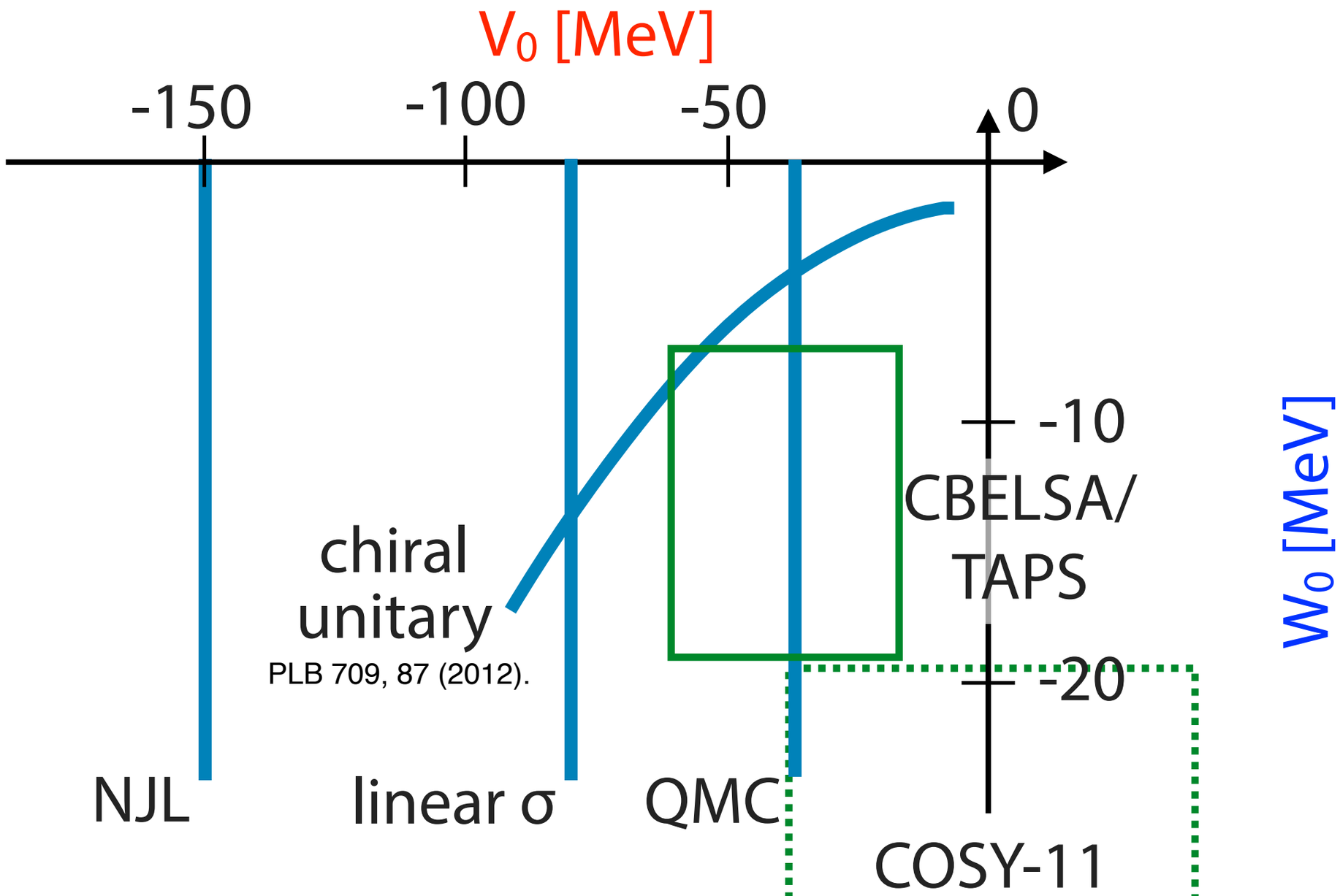

η′-nucleus potential

η′-nucleus optical potential : $V_{\eta'} = (V_0 + iW_0)\frac{\rho(r)}{\rho_0}$

$V_0 = \Delta m(\rho_0)$, $W_0 = -\Gamma(\rho_0)/2$

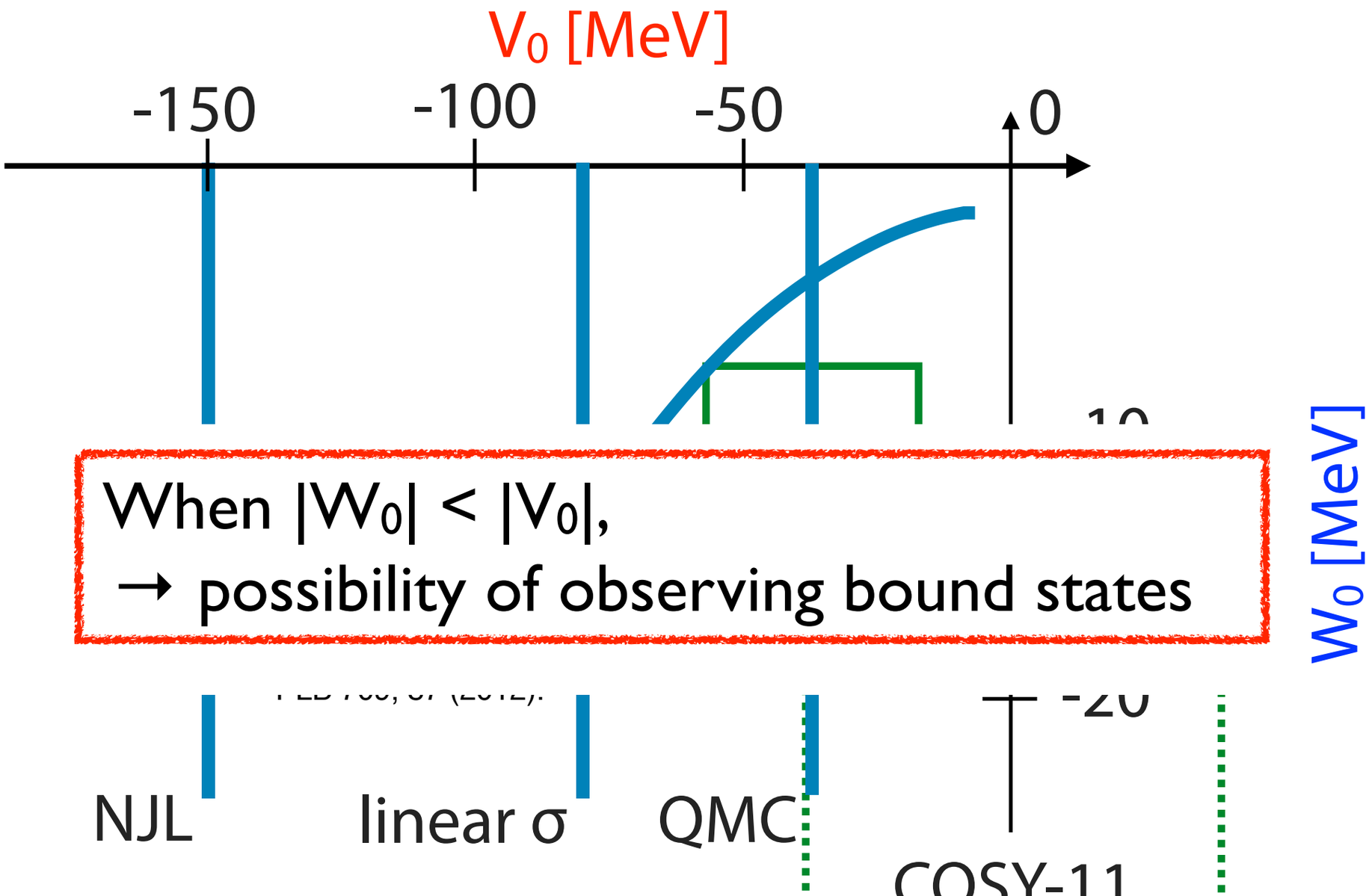

When $|W_0| < |V_0|$,
→ possibility of observing bound states

Missing-mass spectroscopy of $^{12}C(p,d)$ reaction

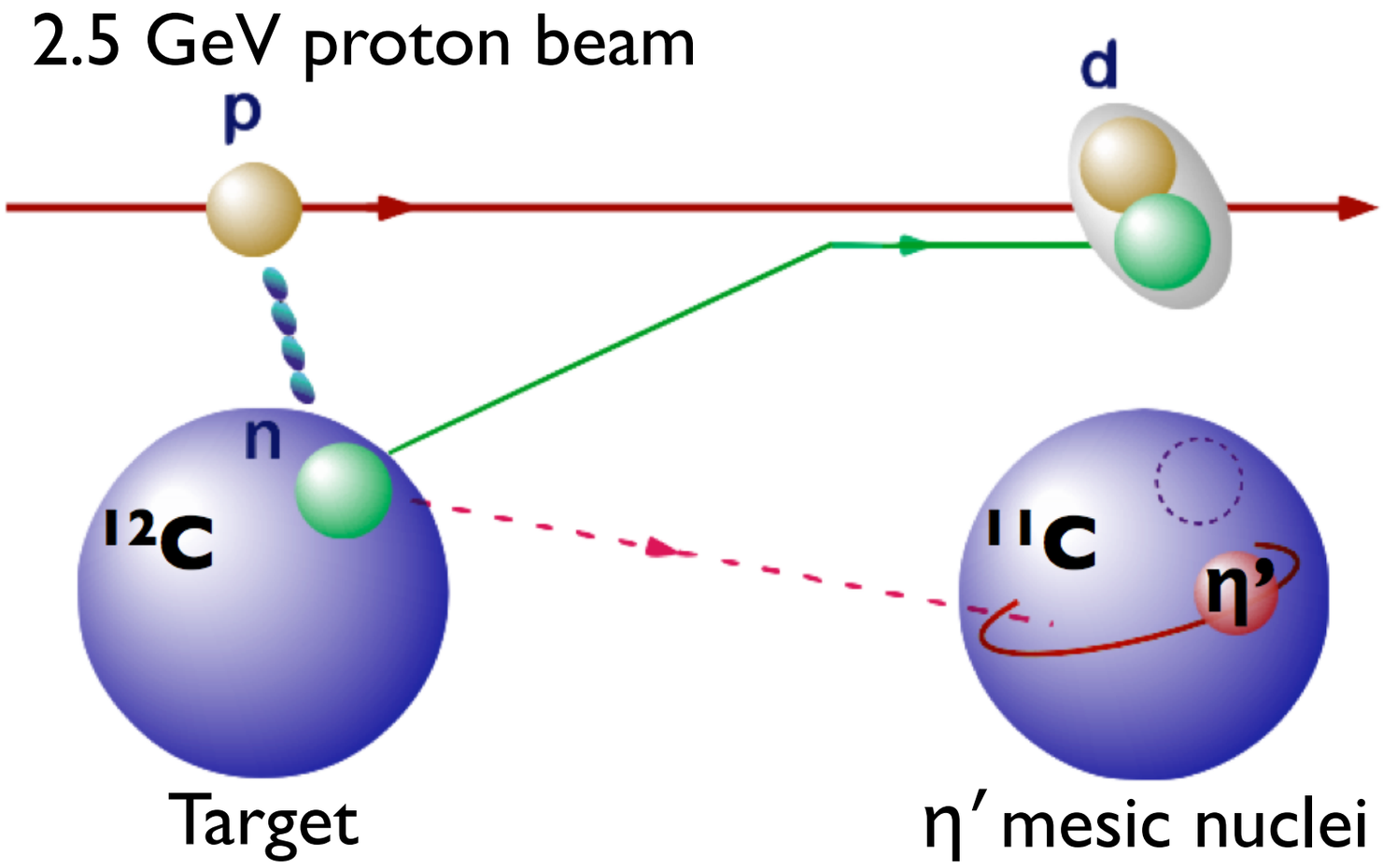

Deuteron momentum measured by FRS

⬇

Missing mass

K. Itahashi *et al.*,
PTP 128, 601(2012)

1st run (Aug. 2014) : inclusive measurement of $^{12}C(p,d)$ reaction

Missing-mass spectroscopy of $^{12}C(p,d)$ reaction

2.5 GeV proton beam

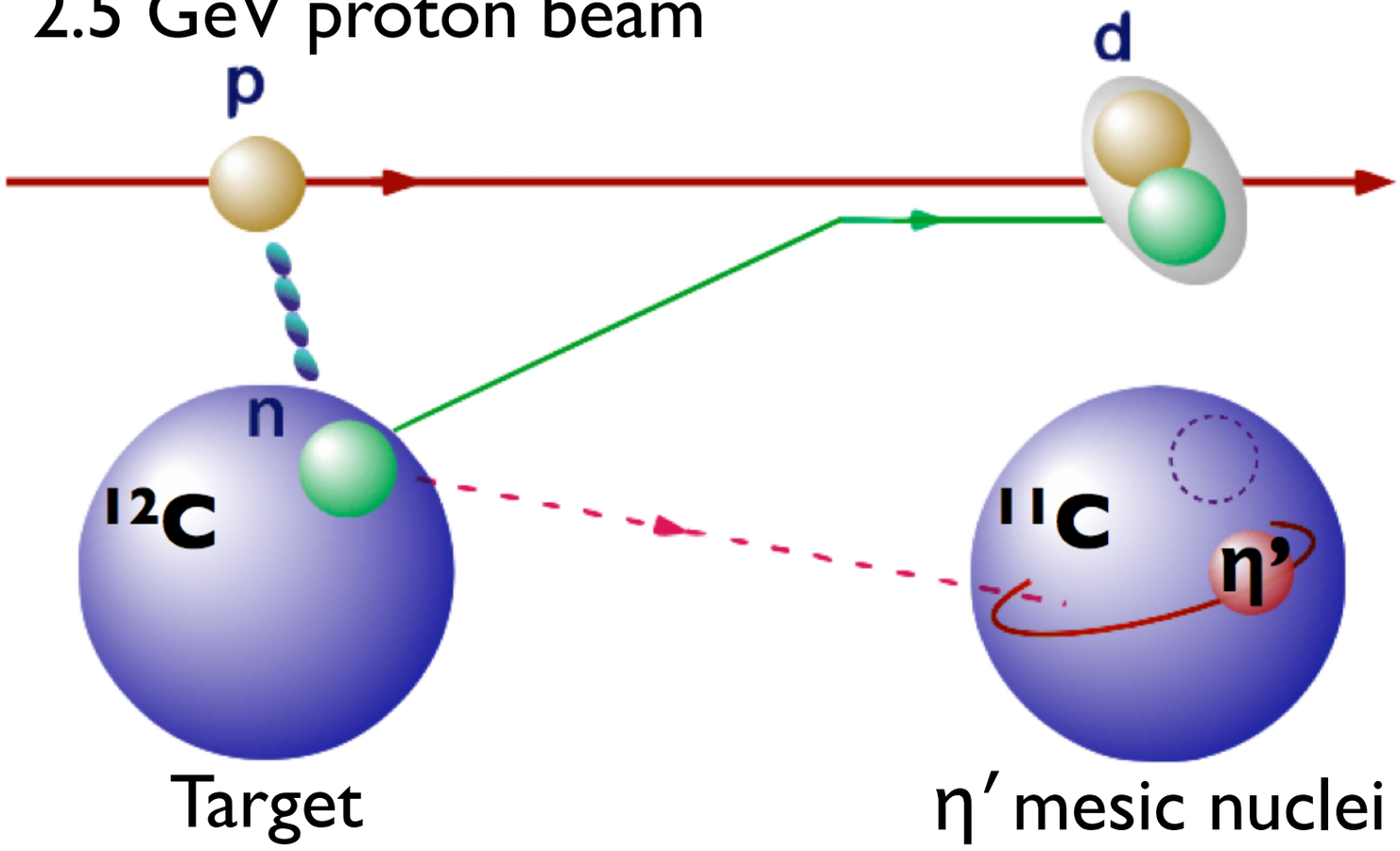

Target

η′ mesic nuclei

Deuteron momentum measured by FRS

⬇

Missing mass

K. Itahashi *et al.*, PTP 128, 601(2012)

1st run (Aug. 2014) : inclusive measurement of $^{12}C(p,d)$ reaction

- overall structure w/o assuming decay process
- S/B ratio $\lesssim O(1/100)$ due to BG processes (e.g., $p+N \rightarrow d+\pi$'s)

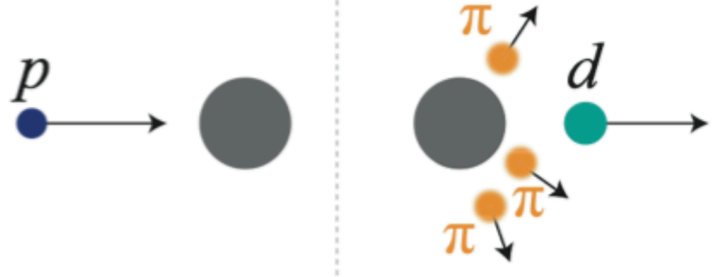

high statistical sensitivity is essential

Theoretically calculated formation spectra

- momentum transfer ~400 MeV/c at T_p = 2.5 GeV
- enhanced excited states near η′ emission threshold

η′ nucleus optical potential :

$$V_{\eta'} = (V_0 + iW_0)\frac{\rho(r)}{\rho_0}$$

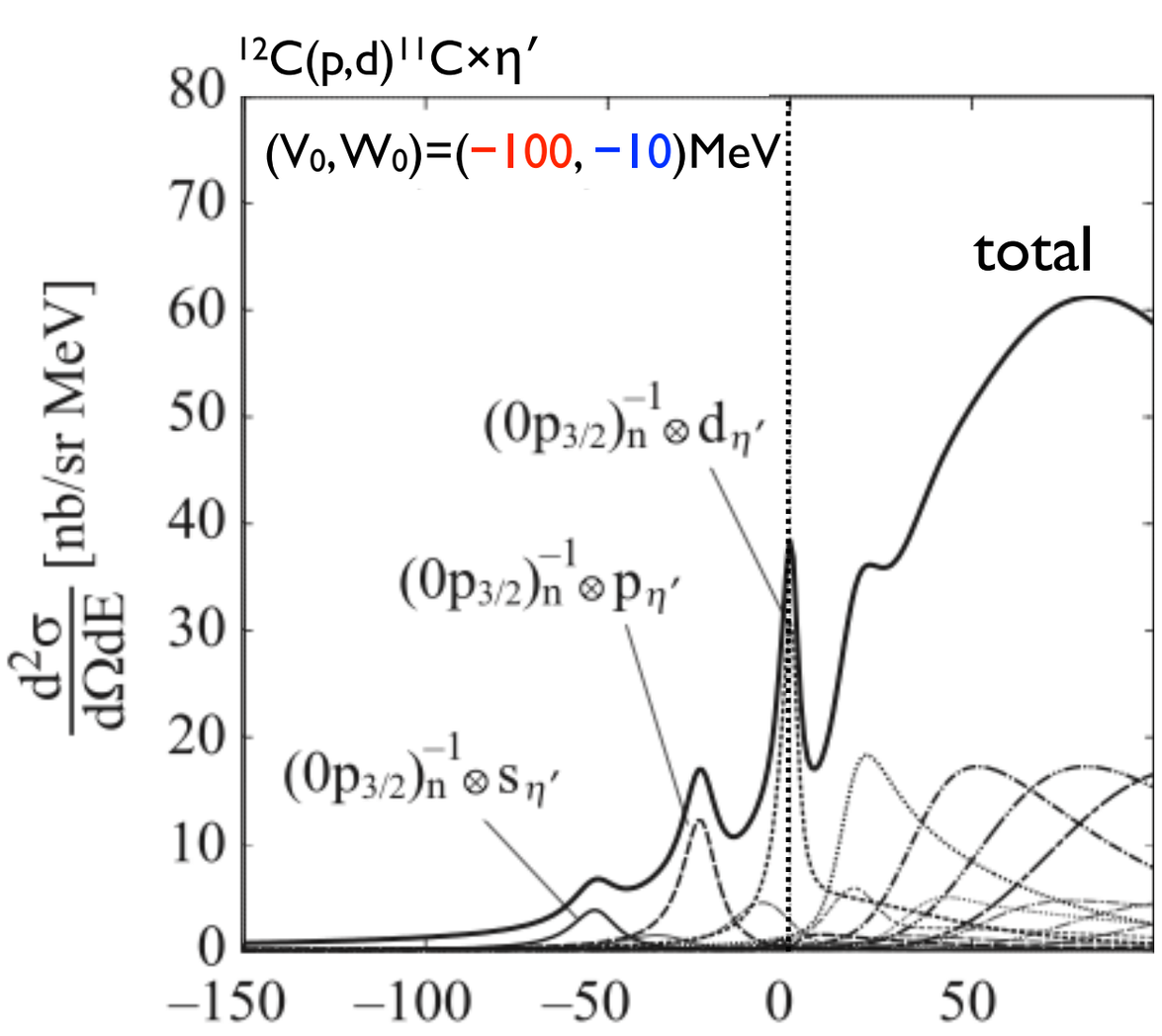

H.Nagahiro et al.,
PRC 87 (2013) 045201.

^{11}C+η′ threshold

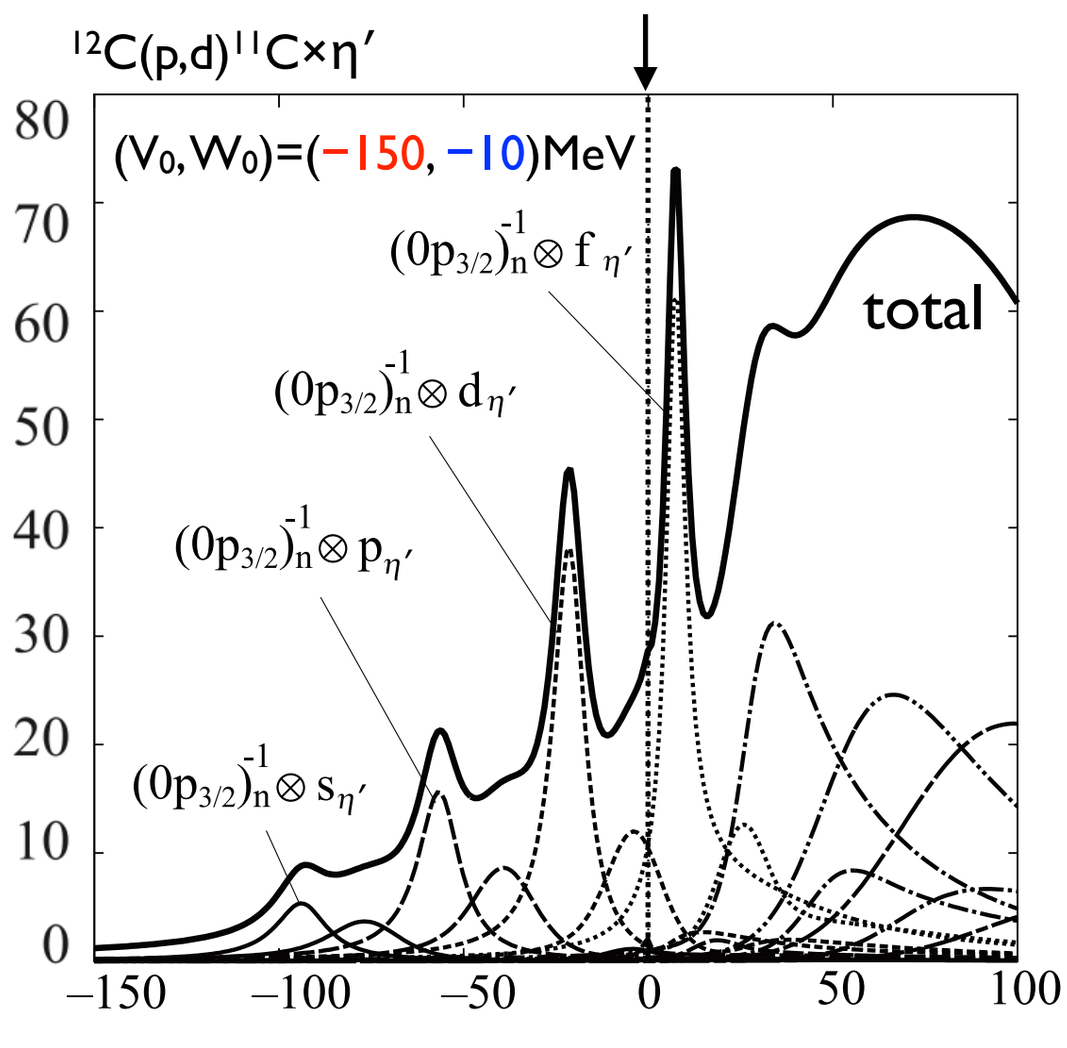

GSI facilities

- SIS-18 : 2.5 GeV proton beam available
- FRS : high-resolution spectrometer + (instrumental) BG rejection

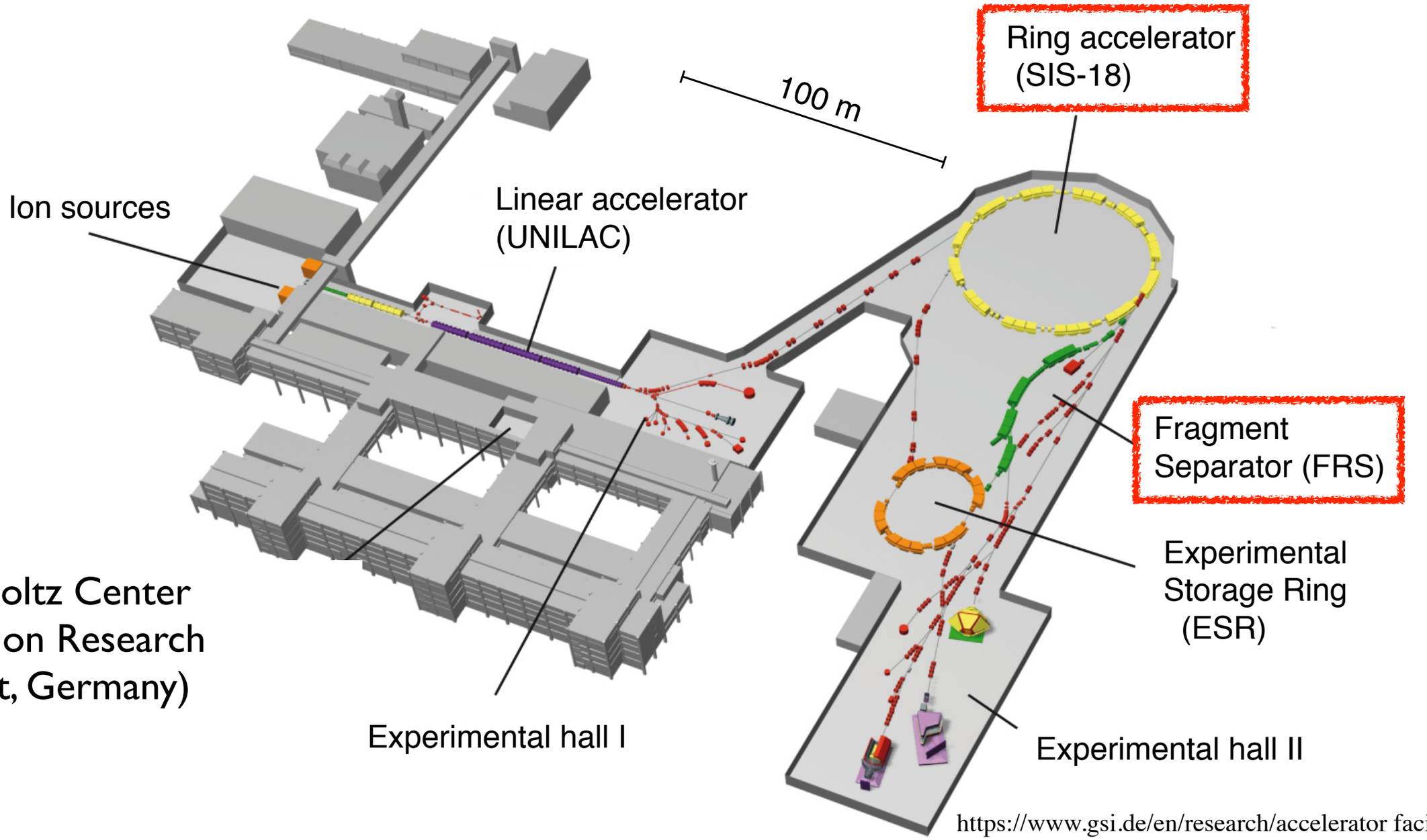

GSI Helmholtz Center
for Heavy Ion Research
(Darmstadt, Germany)

https://www.gsi.de/en/research/accelerator facility.htm

Experimental setup at FRS

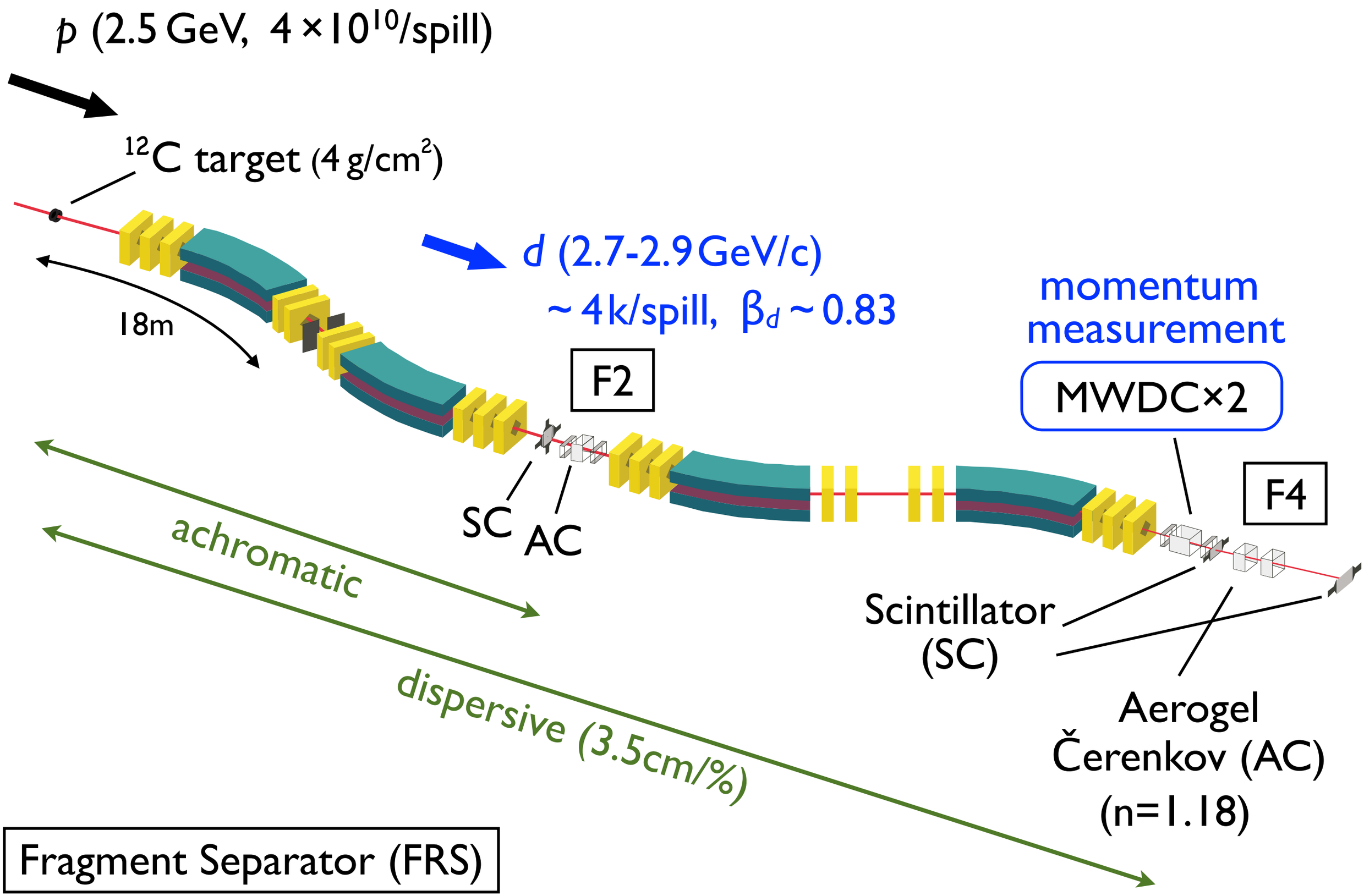

Experimental setup at FRS

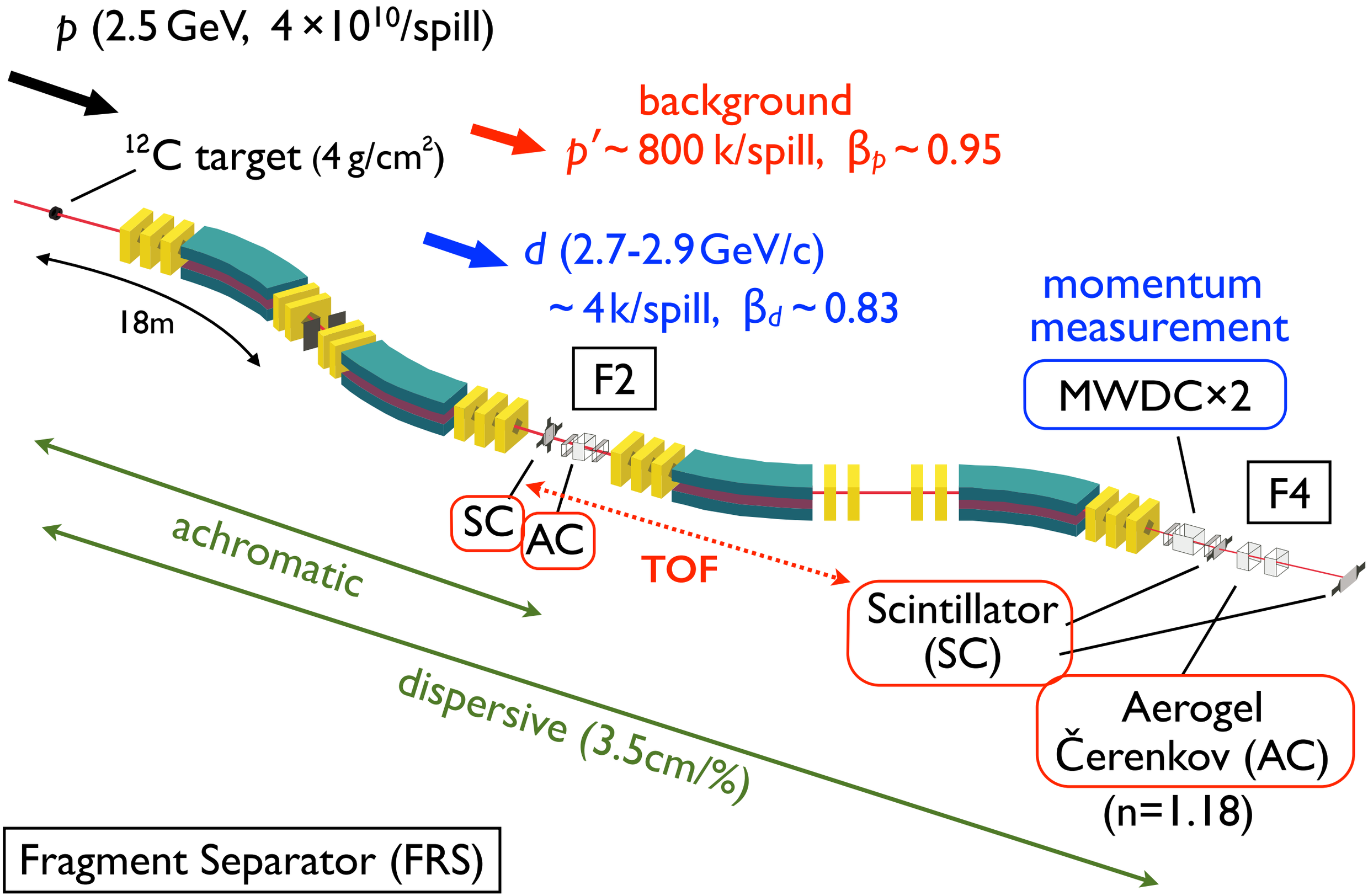

Outline of data analysis

Deuteron identification

- TOF(F2-F4)-based DAQ trigger
- accidental multi-hit rejection by waveform analysis
- TOF(F2-F4) analysis

- proton contamination ~ $O(10^{-4})$ level
- deuteron efficiency ~ 96-97 %

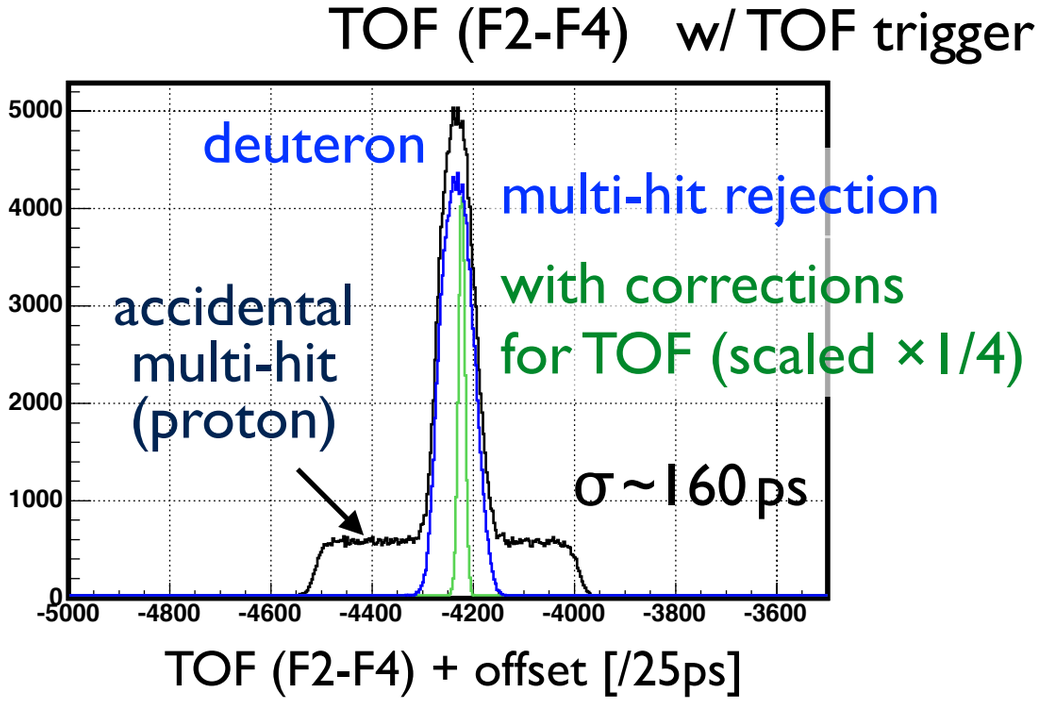

Outline of data analysis

Deuteron identification

- TOF(F2-F4)-based DAQ trigger
- accidental multi-hit rejection by waveform analysis
- TOF(F2-F4) analysis

○ proton contamination ~ $O(10^{-4})$ level
○ deuteron efficiency ~ 96-97 %

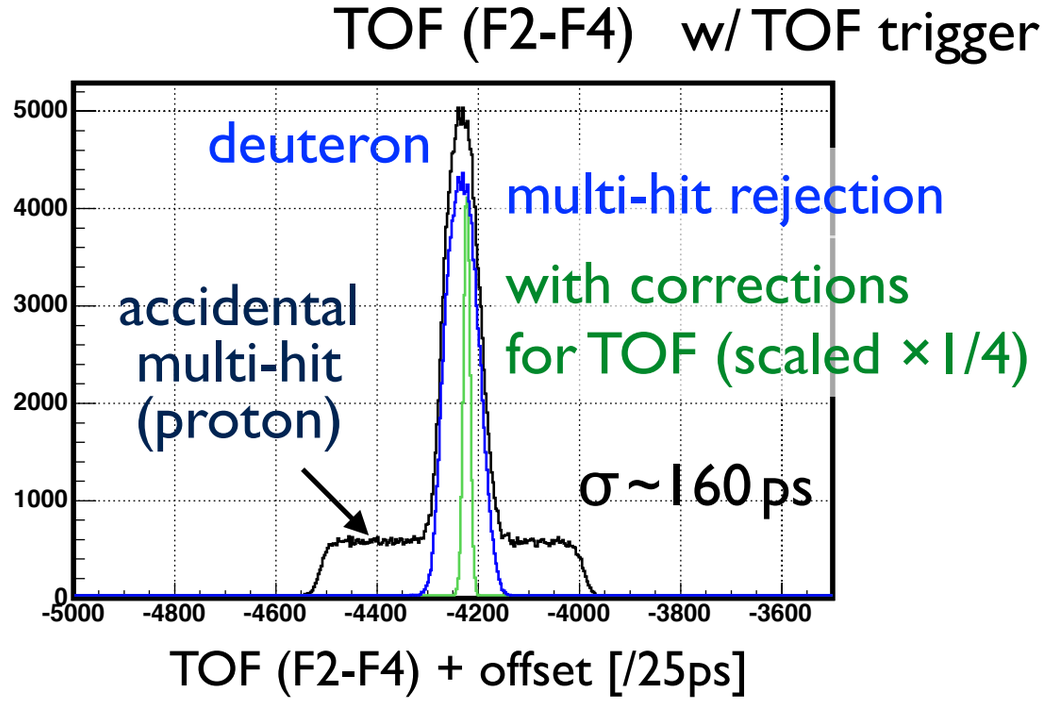

Momentum calibration

- Track reconstruction at F4 focal plane
- Spectrometer calibration by measuring D(*p*,*d*)*p* elastic scattering at 1.6 GeV

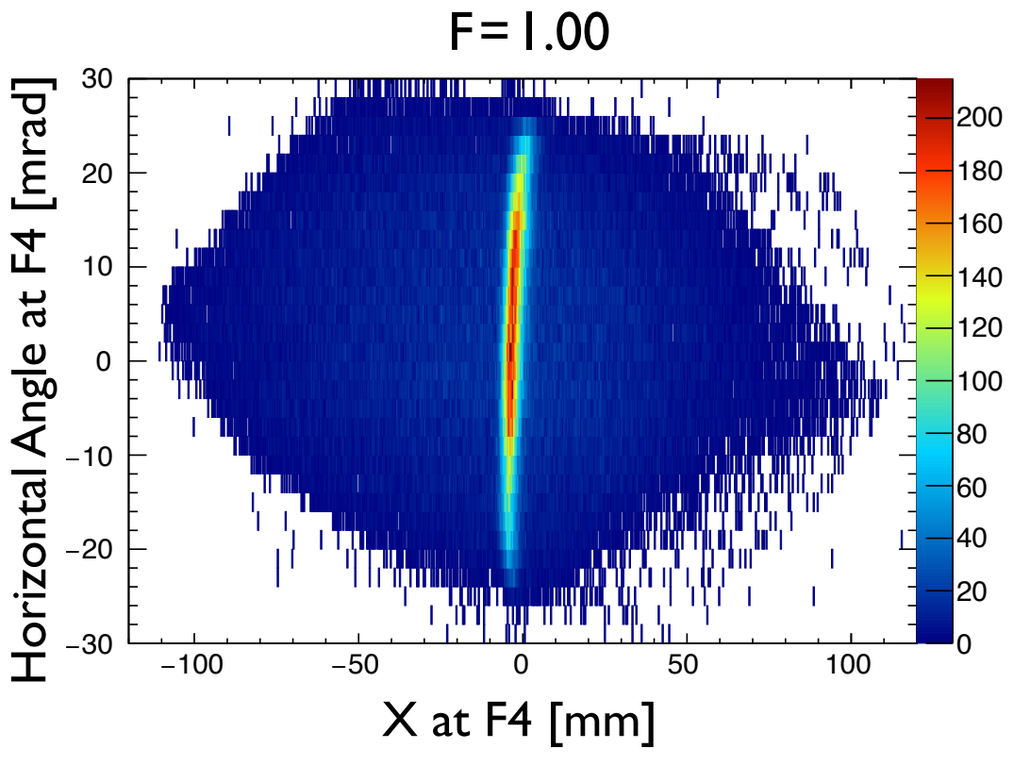

Outline of data analysis

Deuteron identification

- TOF(F2-F4)-based DAQ trigger
- accidental multi-hit rejection by waveform analysis
- TOF(F2-F4) analysis

○ proton contamination ~ $O(10^{-4})$ level
○ deuteron efficiency ~ 96-97 %

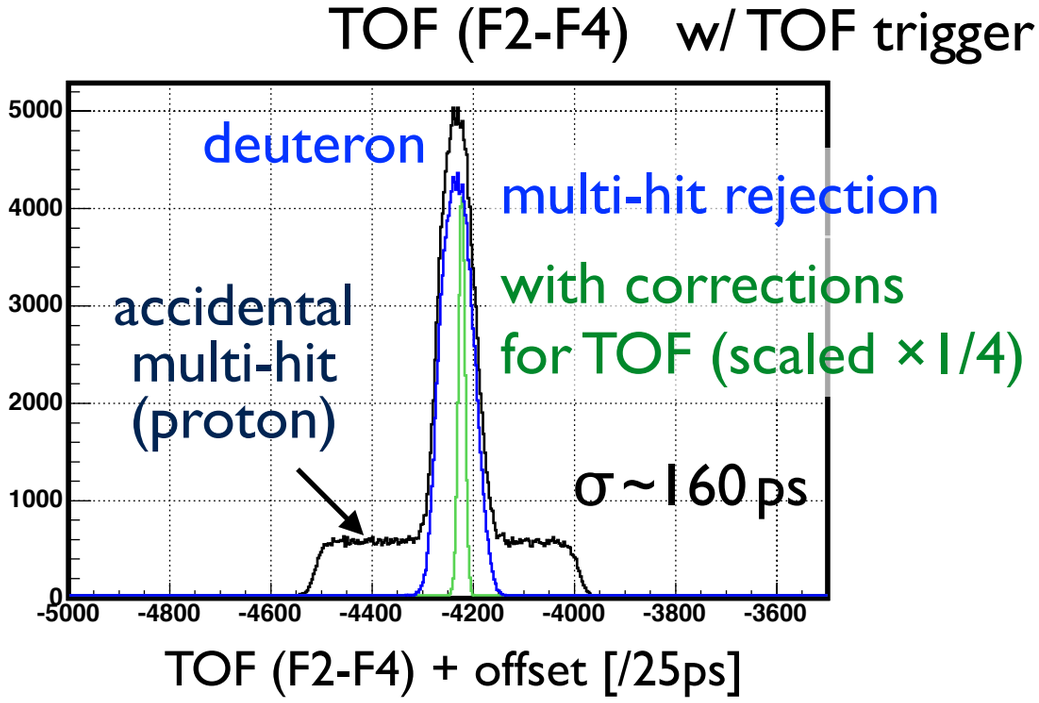

Momentum calibration

- Track reconstruction at F4 focal plane
- Spectrometer calibration by measuring D(*p*,*d*)*p* elastic scattering at 1.6 GeV

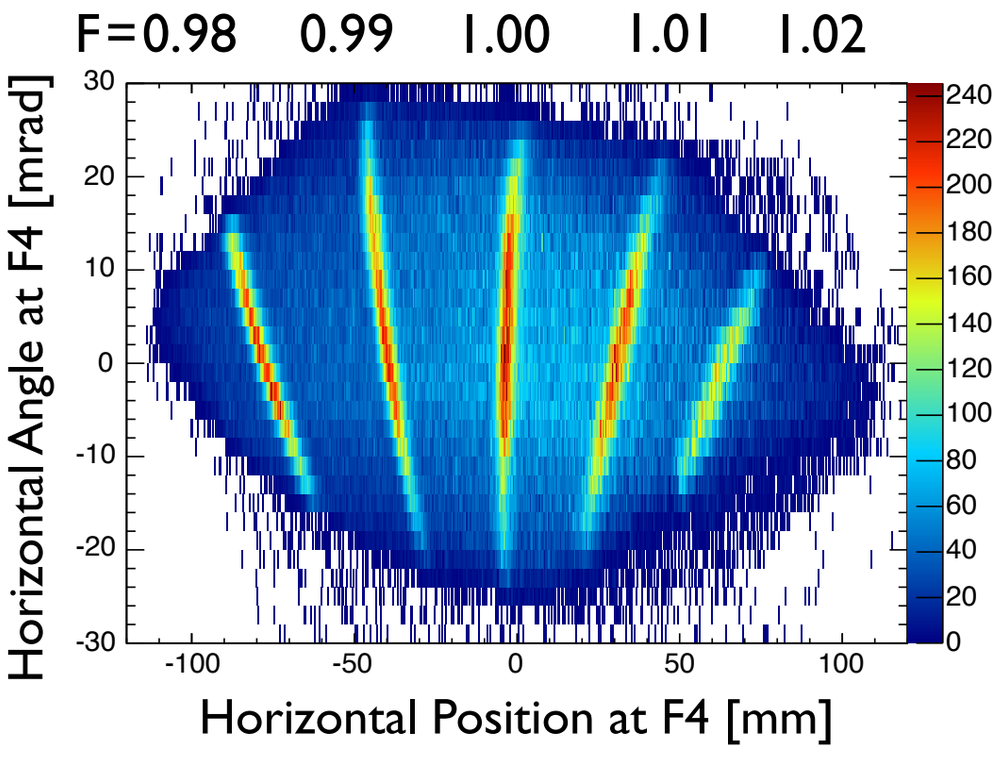

Outline of data analysis

Deuteron identification

- TOF(F2-F4)-based DAQ trigger
- accidental multi-hit rejection by waveform analysis
- TOF(F2-F4) analysis

○ proton contamination ~ $O(10^{-4})$ level
○ deuteron efficiency ~ 96-97 %

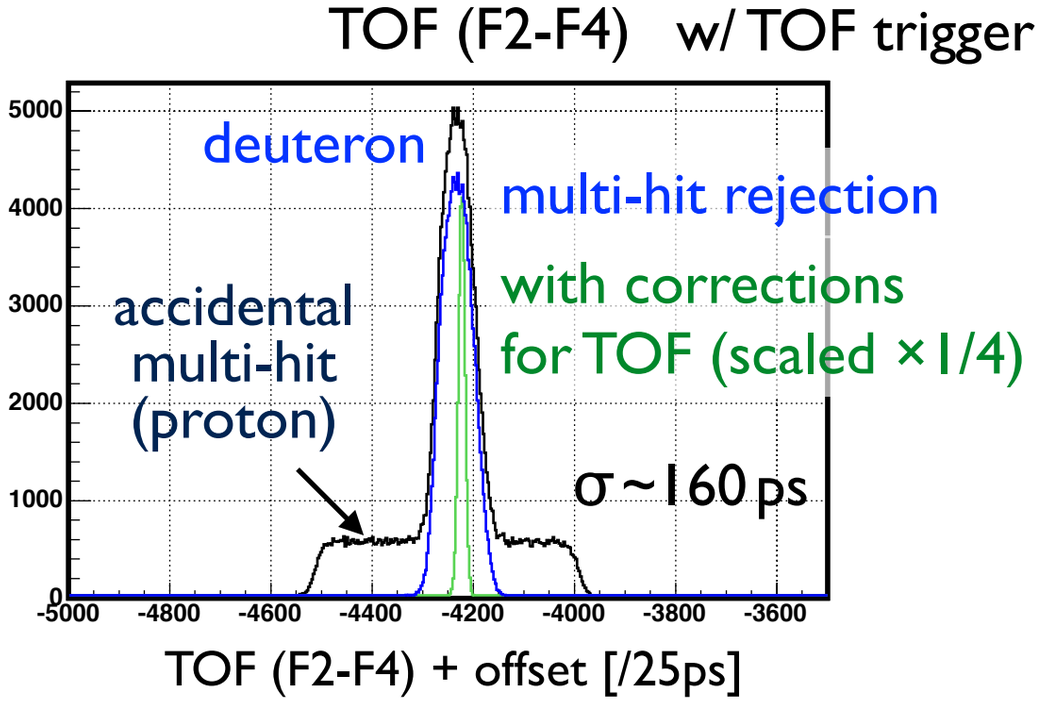

Momentum calibration

- Track reconstruction at F4 focal plane
- Spectrometer calibration by measuring D(*p*,*d*)*p* elastic scattering at 1.6 GeV

Excitation energy of ^{11}C from η′threshold

$$E_{ex} - E_0 = (\text{Missing mass} - M_{^{11}C} - M_{\eta'}) \times c^2$$

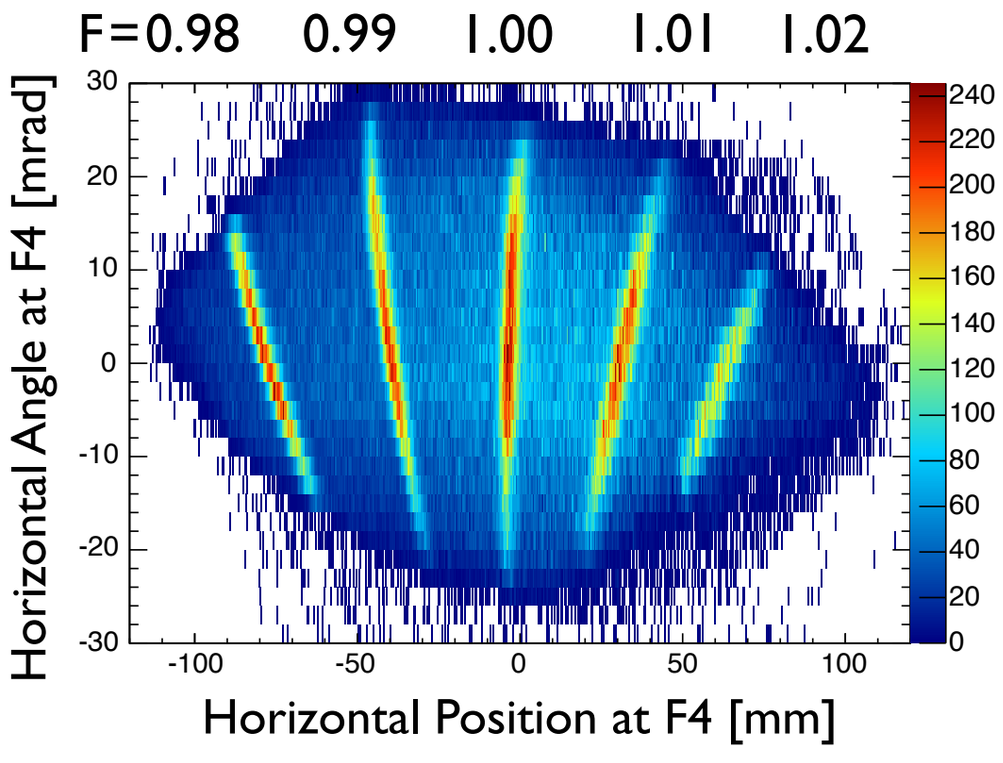

Results — Excitation energy spectrum —

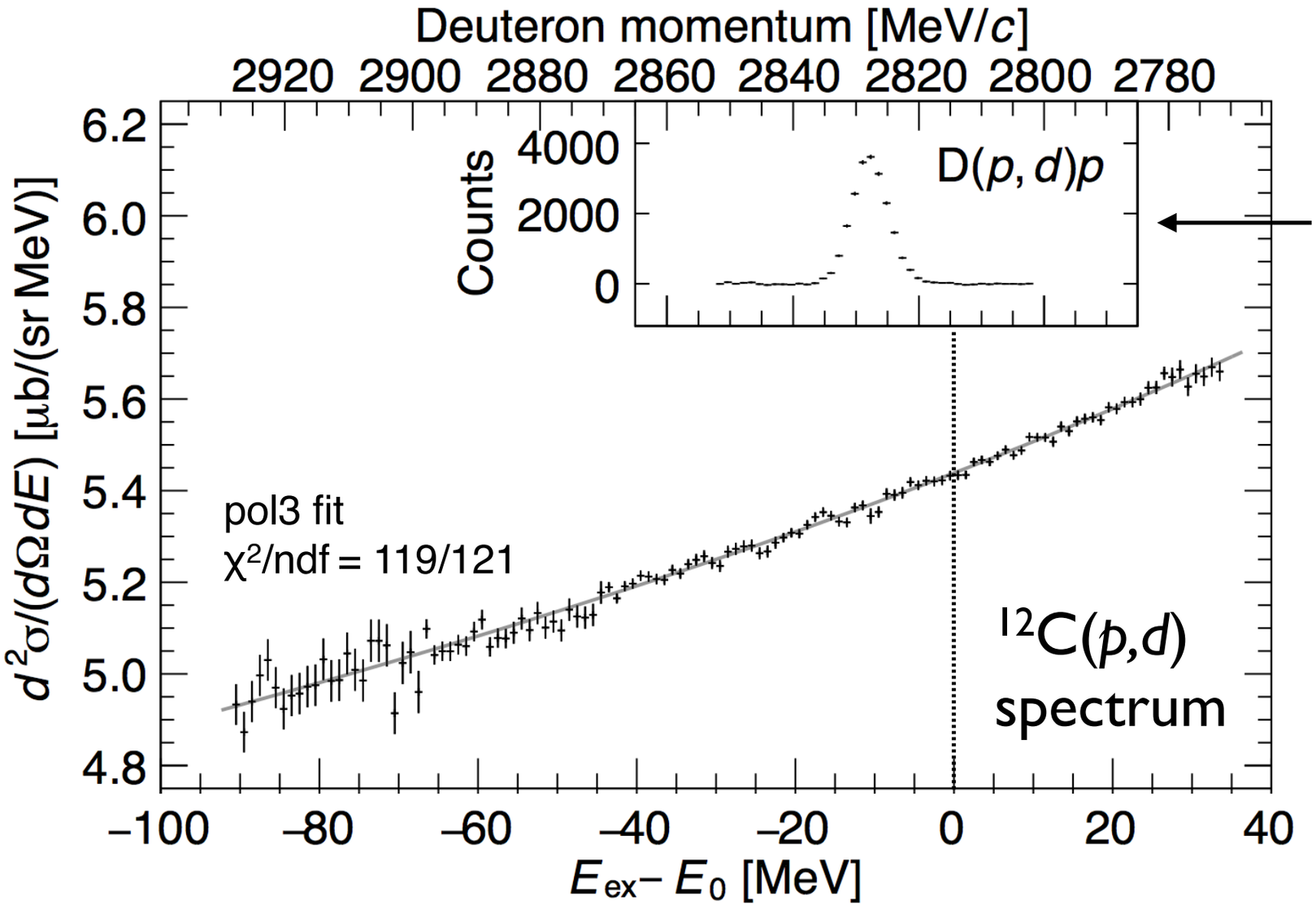

calibration w/ D(*p*,*d*)*p* elastic scattering at T_p = 1.6 GeV

Y. K. Tanaka *et al*,
PRL 117, 202501 (2016)

Results — Excitation energy spectrum —

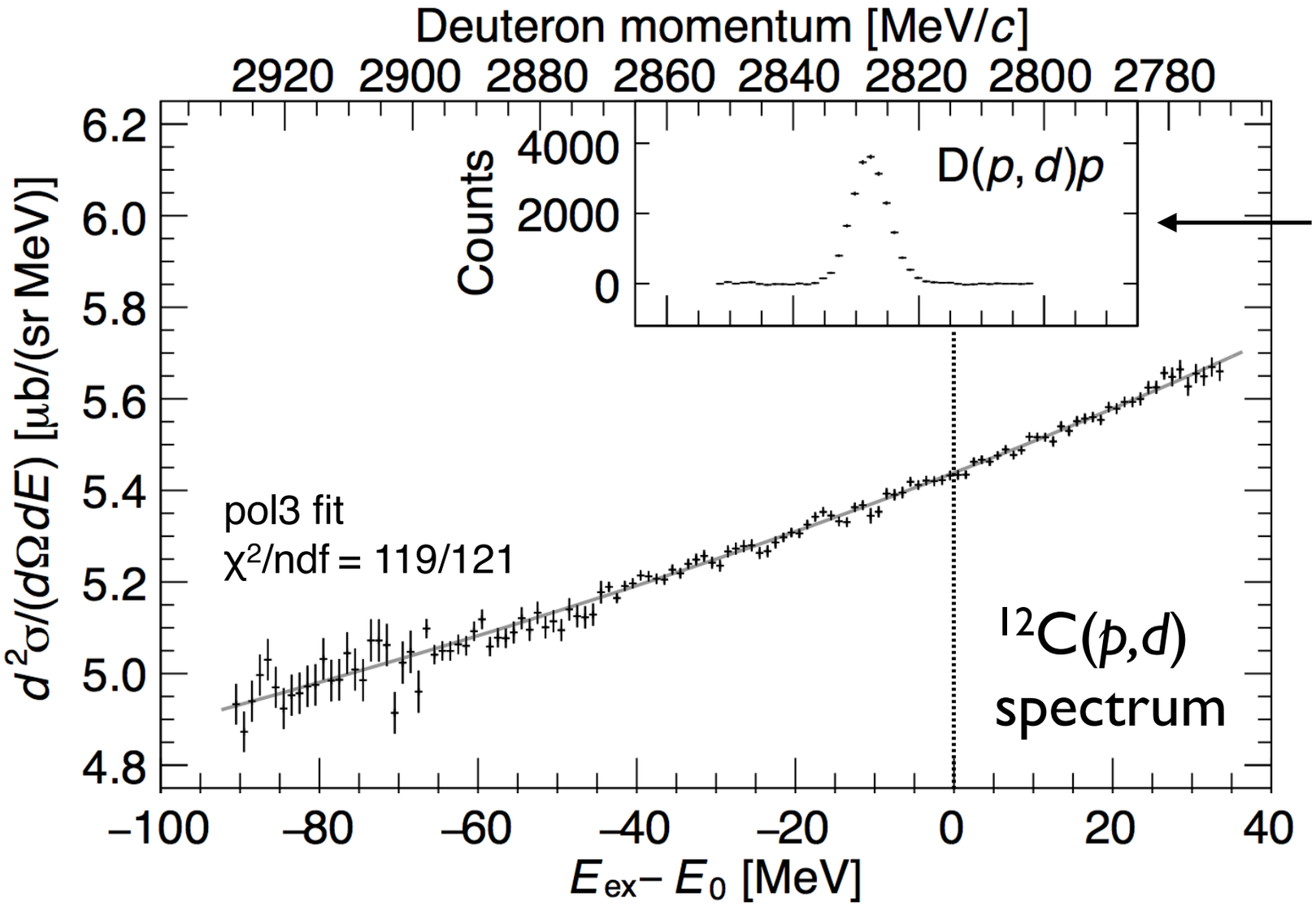

calibration w/ D(*p*,*d*)*p* elastic scattering at T_p = 1.6 GeV

Y. K. Tanaka *et al*,
PRL 117, 202501 (2016)

- good statistical sensitivity ≲ 1% is achieved
- overall (*p*,*d*) cross section consistent with quasi-free multi-π production
- sufficient resolution 2.5 MeV(σ) achieved
- no significant peak structure is observed
  → upper limits for formation cross section of η′ mesic states

Upper limit of formation cross section

Upper limit of Lorentzian-shaped formation cross section

- fit function: $A \times \mathrm{Voigt}(E; E_{test}, \Gamma_{test}, \sigma_{exp}) + \mathrm{Pol3}(E; p_0, p_1, p_2, p_3)$

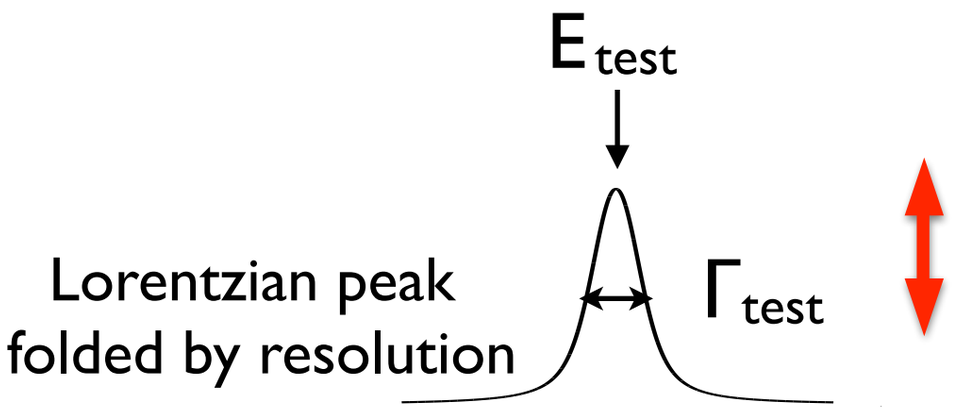

- evaluate upper limit of cross section for fixed (E_{test}, Γ_{test})
- repeat analysis for other (E_{test}, Γ_{test})

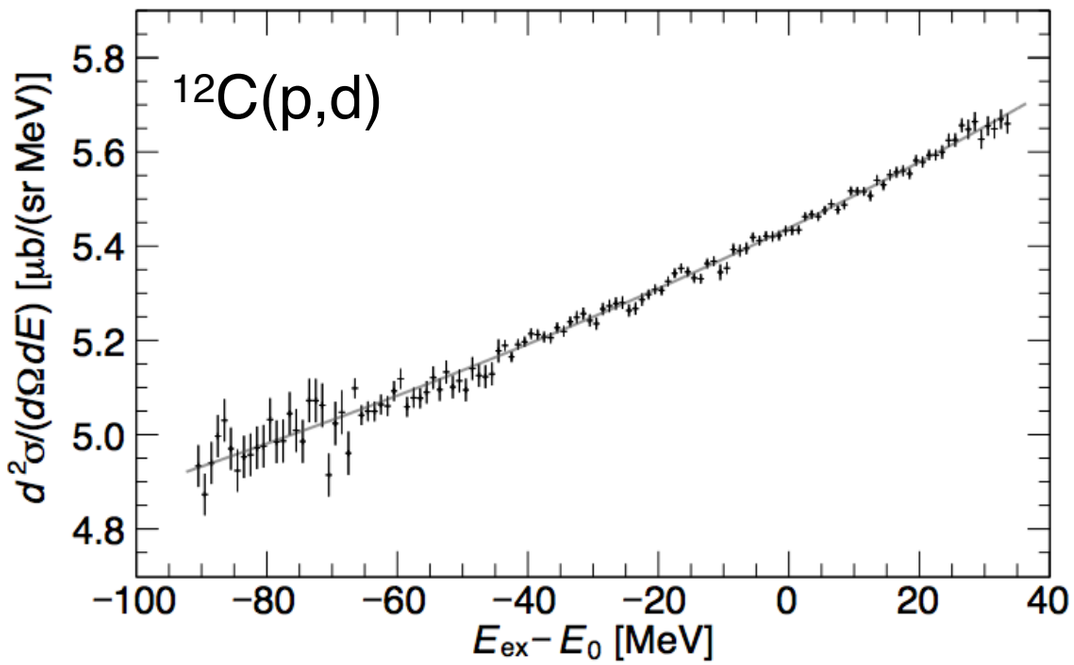

Upper limit of formation cross section

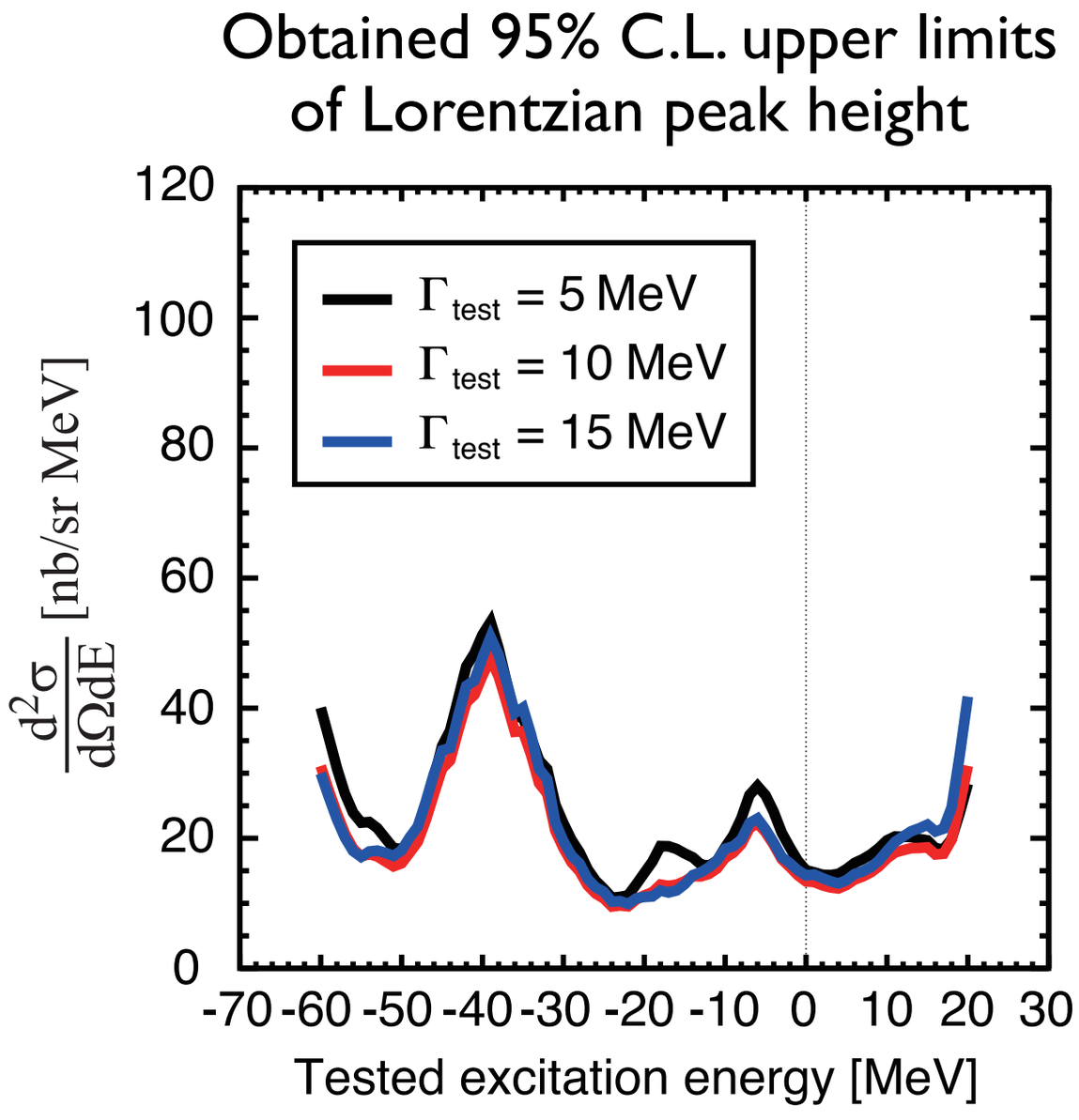

- high statistical sensitivity better than 1% is achieved (as intended)

Upper limit of formation cross section

Obtained 95% C.L. upper limits of Lorentzian peak height

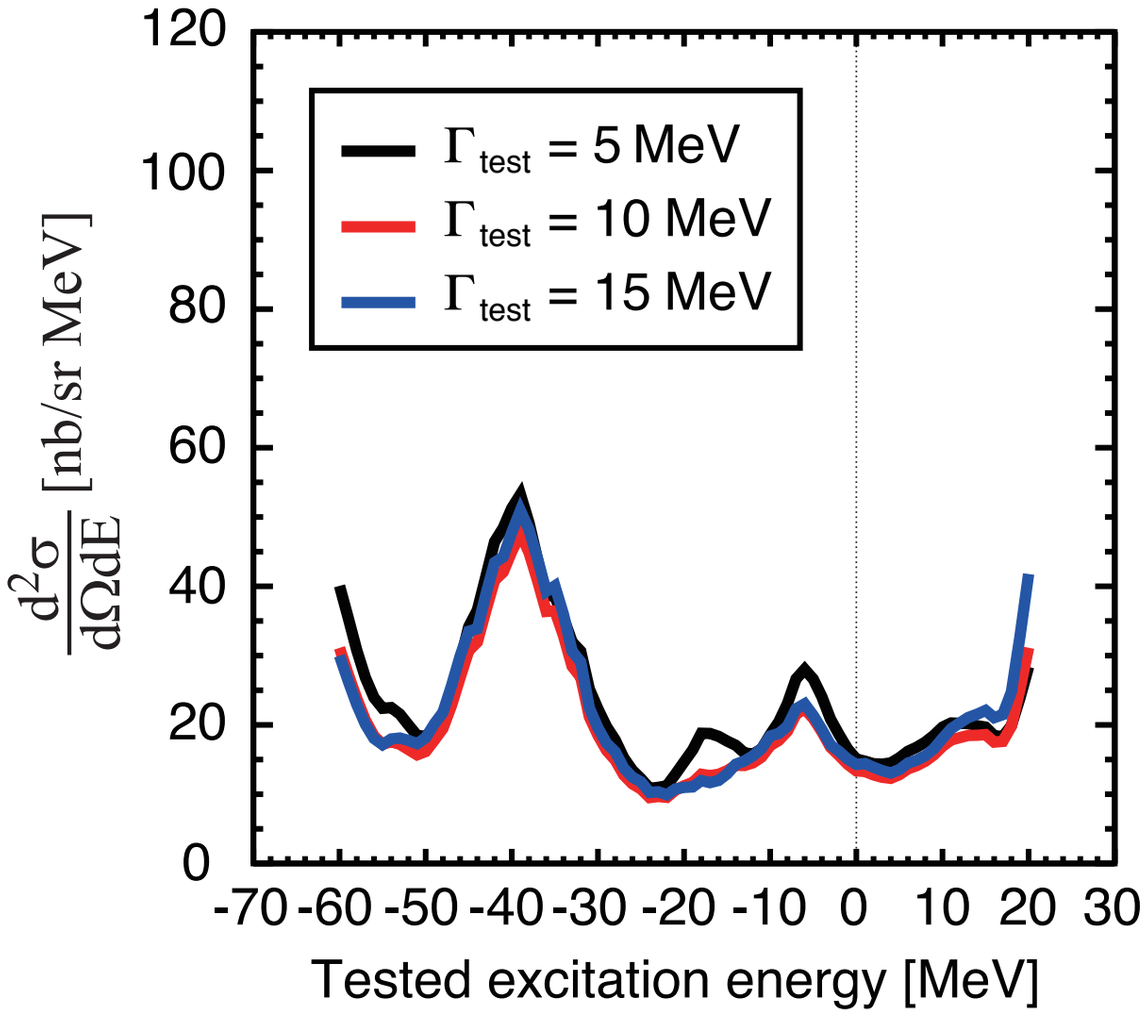

Theoretically expected spectrum for $(V_0, W_0) = (-150, -10)$ MeV

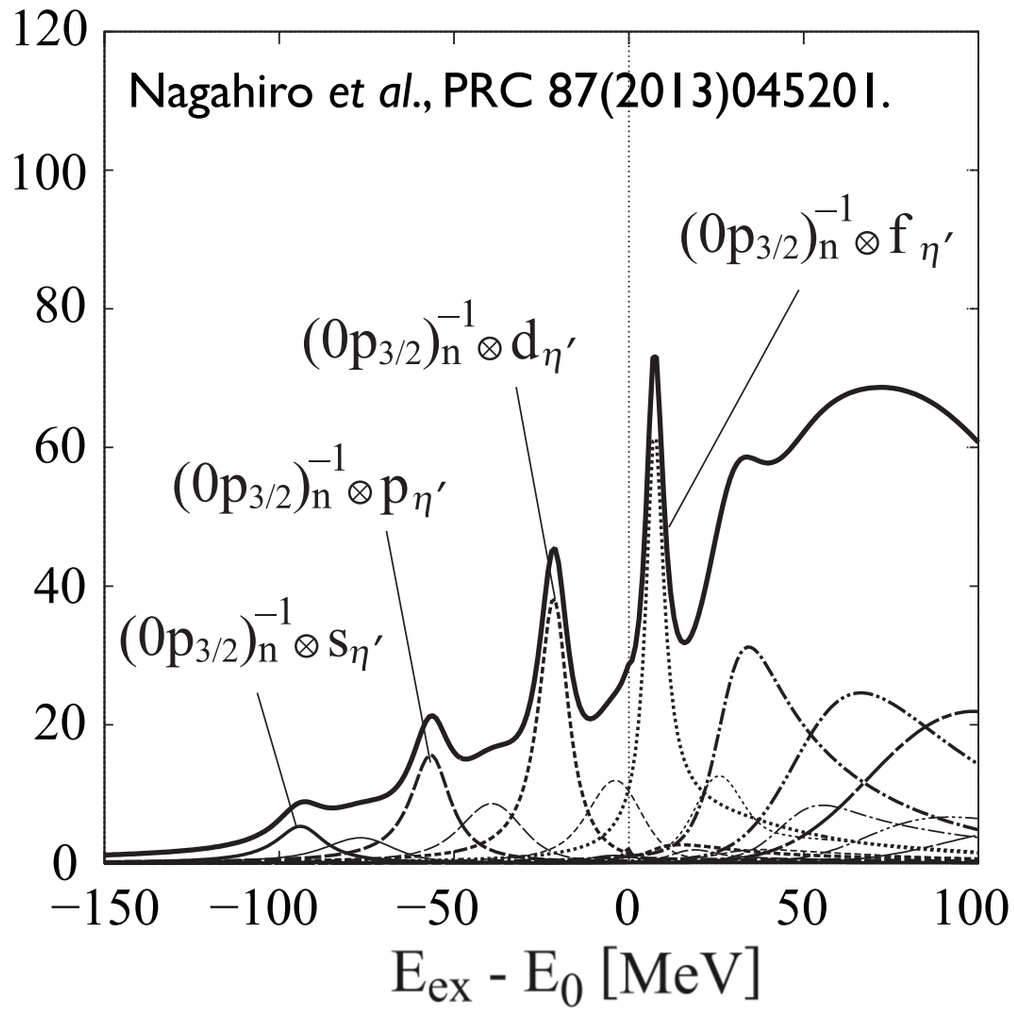

- high statistical sensitivity better than 1% is achieved (as intended)
- ~40 nb/(sr·MeV) peak expected for $(V_0, W_0) = (-150, -10)$ MeV is excluded at 95% C.L.

Upper limit of formation cross section

Obtained 95% C.L. upper limits of Lorentzian peak height

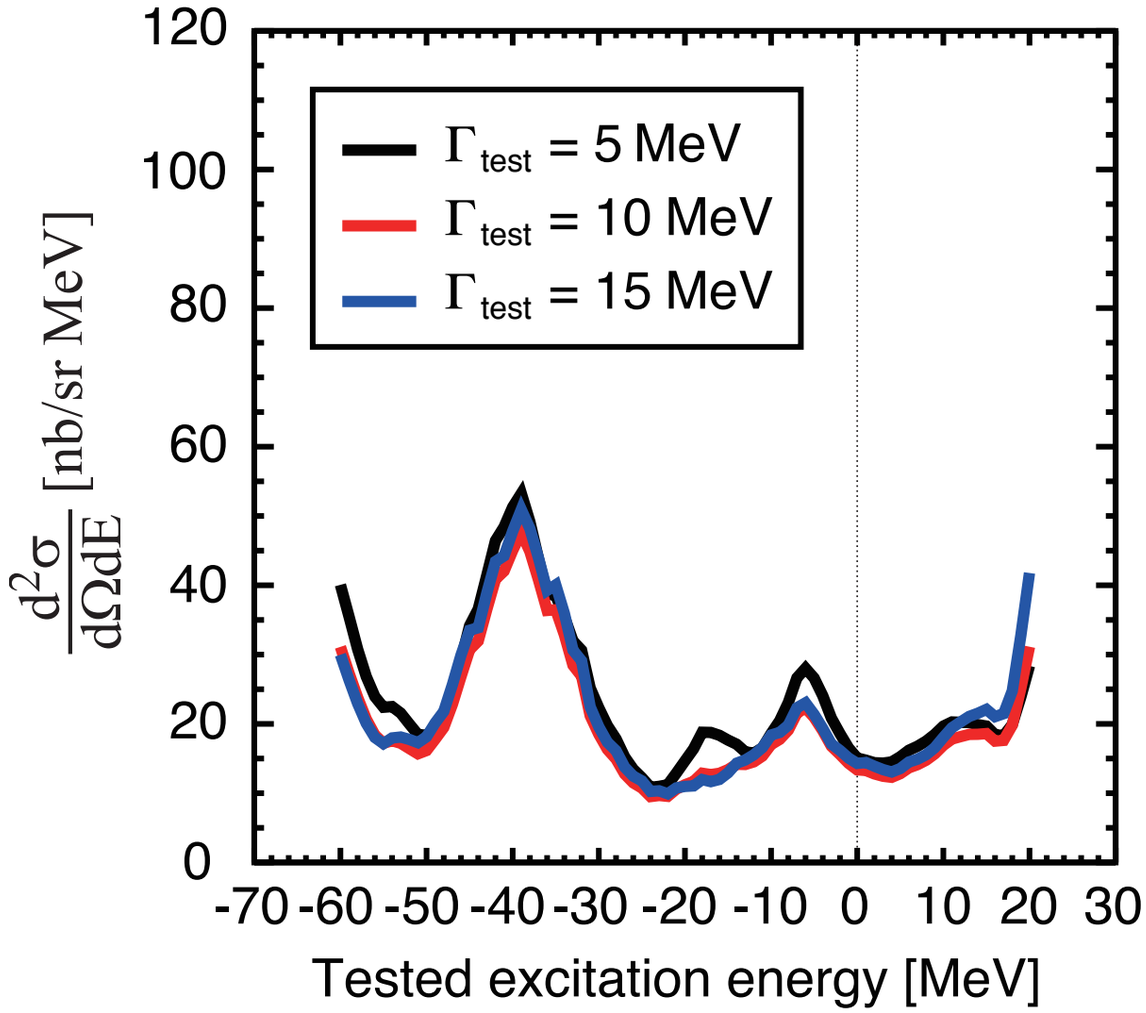

Theoretically expected spectrum for $(V_0, W_0) = (-100, -10)$ MeV

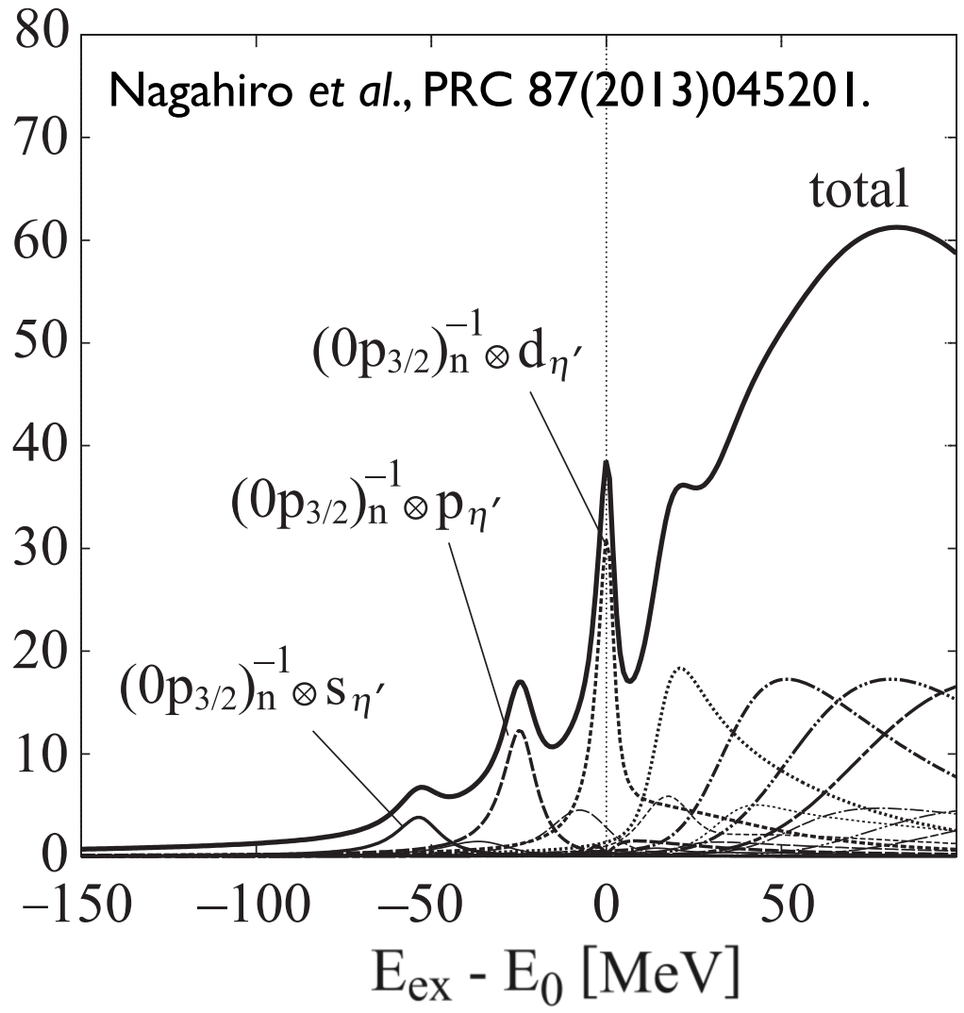

- high statistical sensitivity better than 1% is achieved (as intended)
- ~ 30 nb/(sr·MeV) peak expected for $(V_0, W_0) = (-100, -10)$ MeV is excluded at 95% C.L.

Upper limit of formation cross section

Obtained 95% C.L. upper limits of Lorentzian peak height

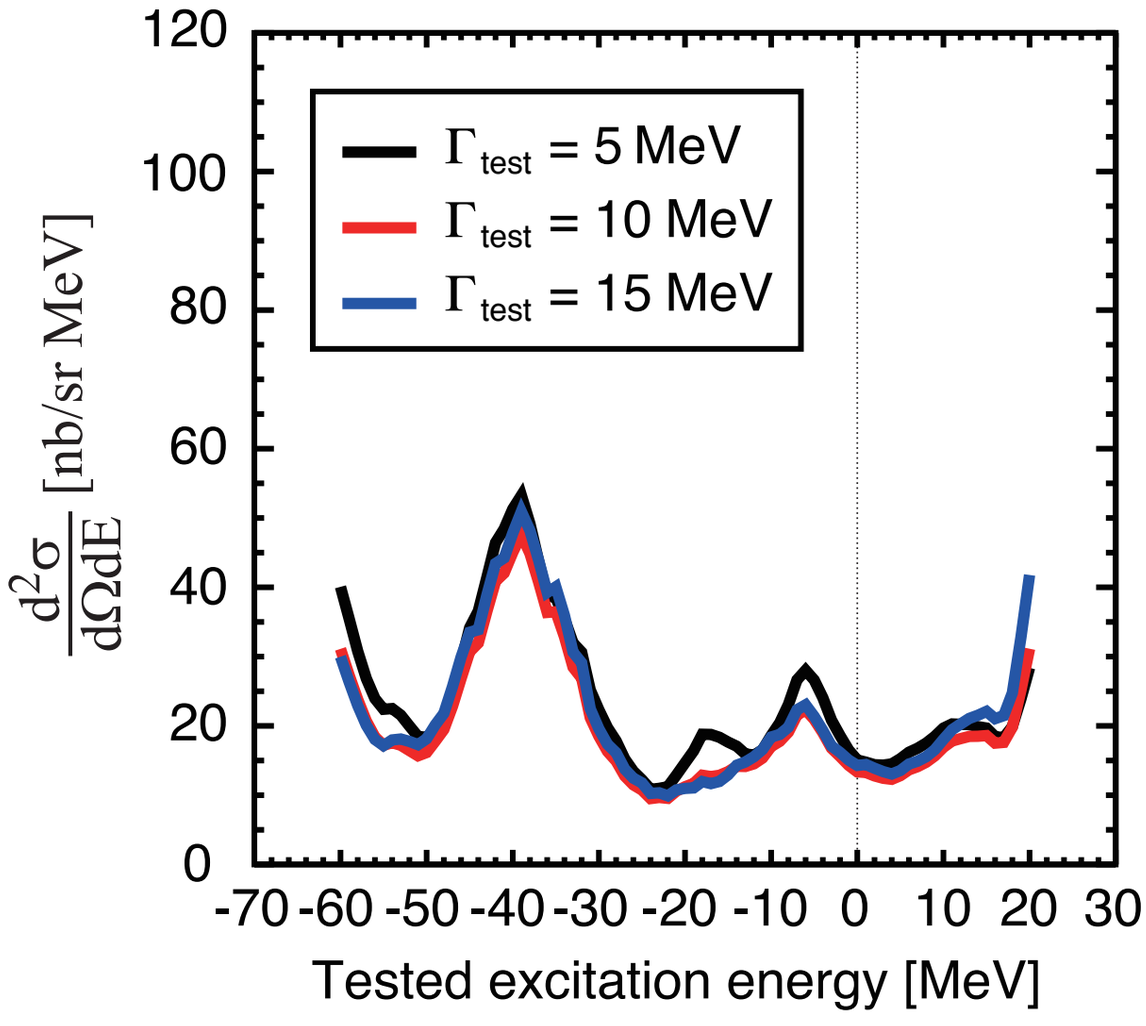

Theoretically expected spectrum for $(V_0, W_0) = (-50, -10)$ MeV

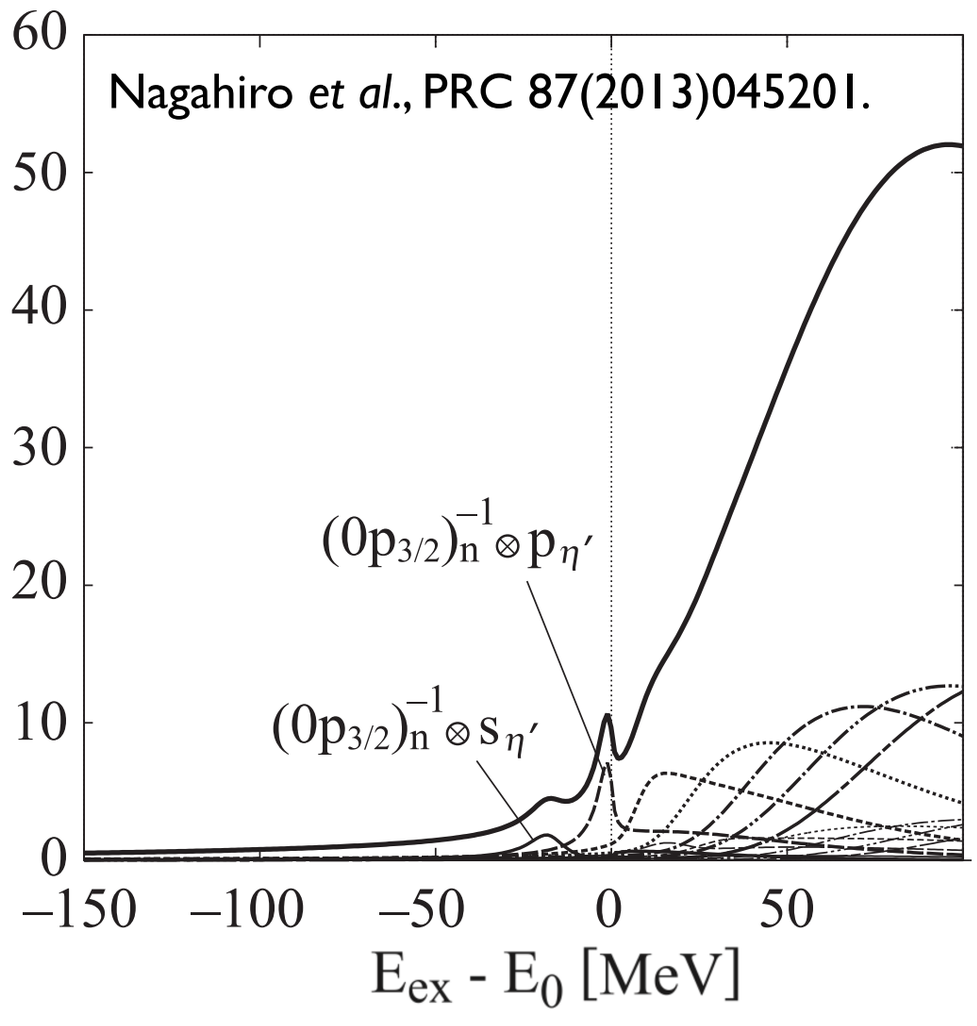

- high statistical sensitivity better than 1% is achieved (as intended)
- ~ 10nb/(sr·MeV) peak expected for $(V_0, W_0) = (-50, -10)$ MeV is not in conflict with present data

Comparison with theoretical spectra

Analysis of possible scale μ for theoretically-calculated spectrum

- fit function : $\mu \times (d^2\sigma/d\Omega dE)^{\text{theory}\times\text{resolution}} + \text{Pol3}(E; p_0,p_1,p_2,p_3)$
- upper limit of μ at 95% C.L.
- analysis repeated for various (V_0, W_0)

$$V_{\eta'} = (V_0 + iW_0)\frac{\rho(r)}{\rho_0}$$

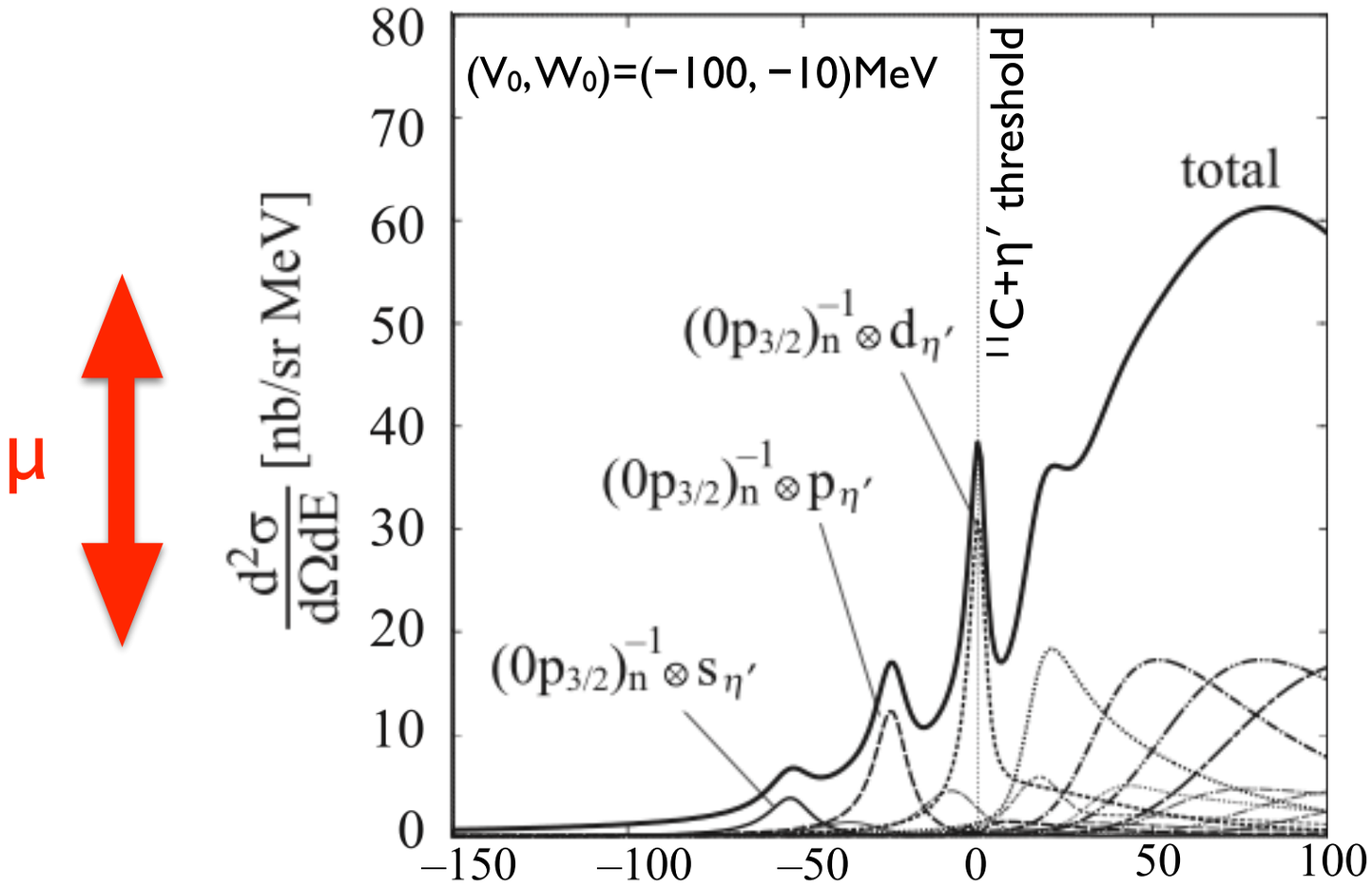

H.Nagahiro *et al.*,
PRC 87, 045201 (2013)

Comparison with theoretical spectra

Analysis of possible scale μ for theoretically-calculated spectrum

- fit function: $\mu \times (d^2\sigma/d\Omega dE)^{\text{theory}\times\text{resolution}} + \text{Pol3}(E; p_0,p_1,p_2,p_3)$
- upper limit of μ at 95% C.L.
- analysis repeated for various (V_0, W_0)

$$V_{\eta'} = (V_0 + iW_0)\frac{\rho(r)}{\rho_0}$$

limit of μ (contour plot)

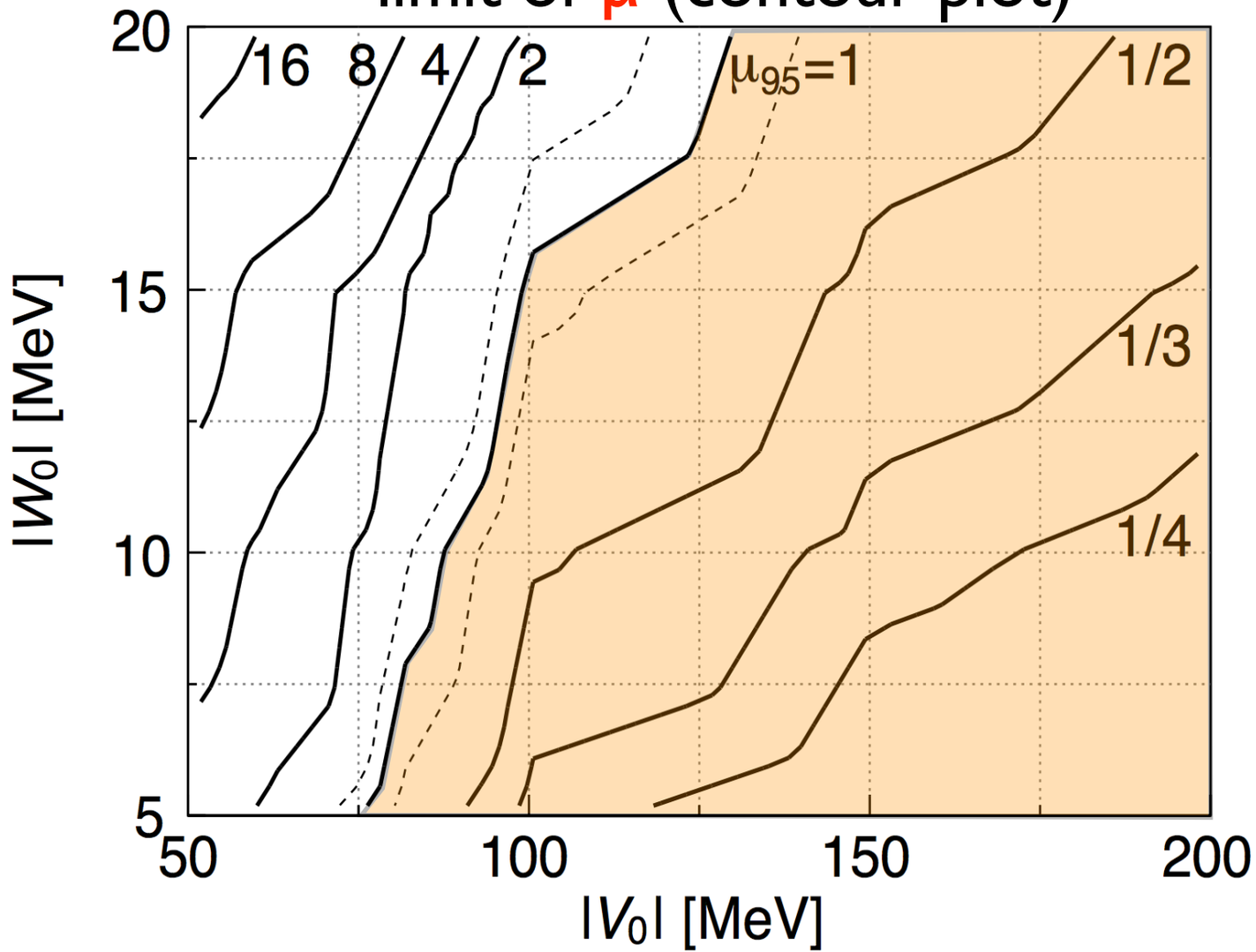

(V_0, W_0) with $\mu_{\text{limit}} < 1$ is excluded under this comparison

- Strongly attractive potential
  $|V_0| \sim 150$ MeV (NJL)
  is rejected in this analysis
  for $|W_0| < 20$ MeV
- need to extend sensitivity for shallower potential

Y. K. Tanaka *et al*,
PRL 117, 202501 (2016)

Future prospects at GSI/FAIR

Semi-exclusive measurement by tagging decay particles

Background

multi-π production

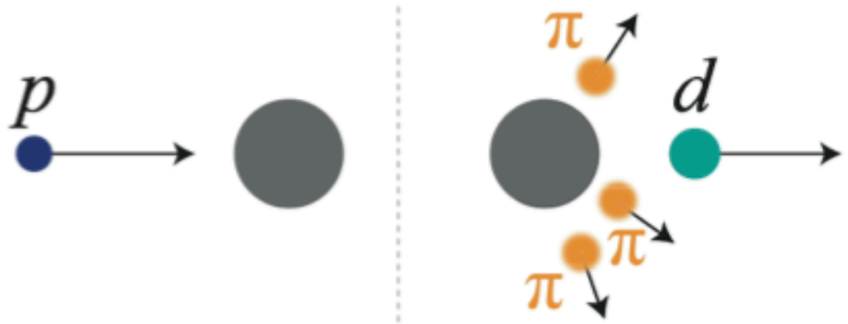

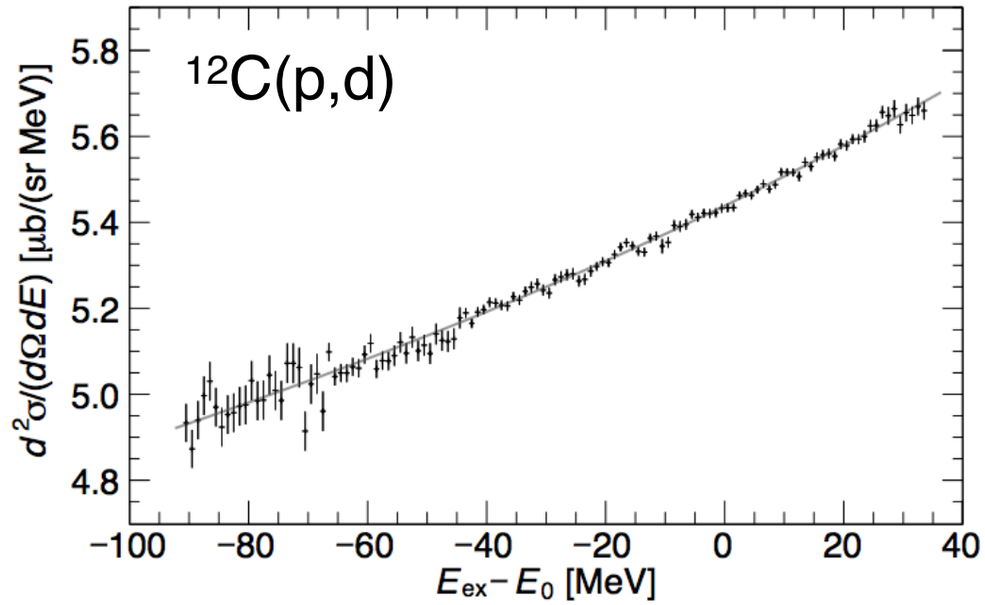

Signal

η′ mesic nuclei formation

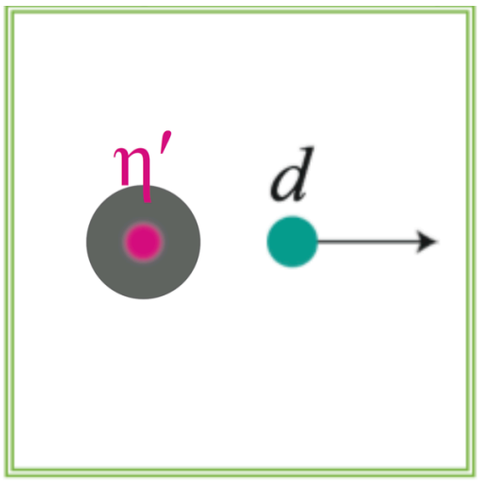

Future prospects at GSI/FAIR

Semi-exclusive measurement by tagging decay particles

Background

multi-π production

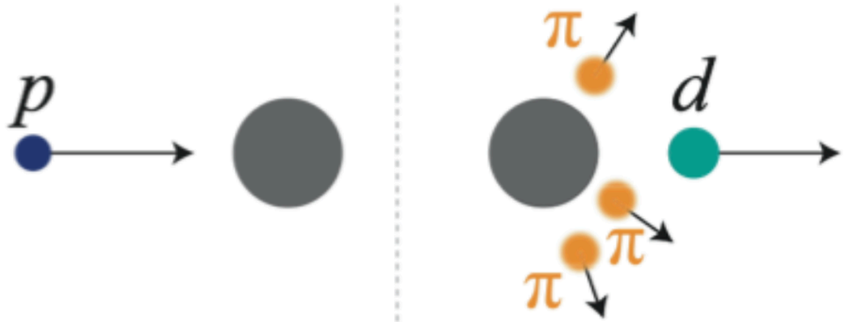

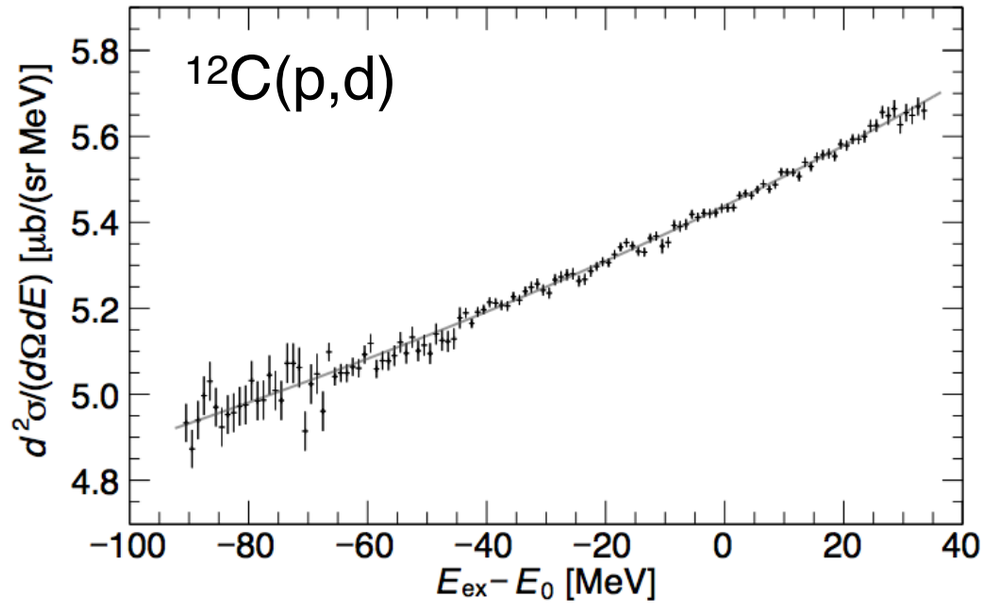

Signal

η′ mesic nuclei formation

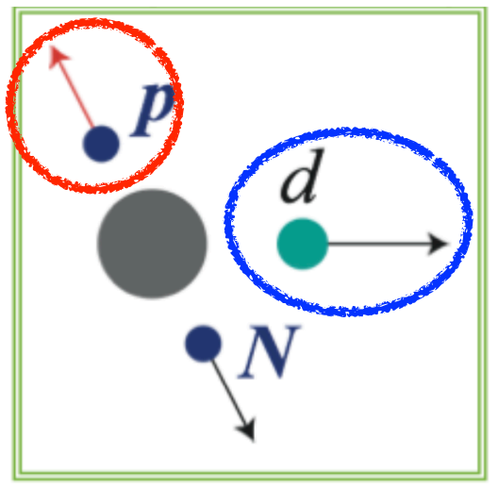

η′*pN*→*pN*

coincidence measurement of

- forward deuteron
- decay proton (~ 1GeV/c)

⬇

S/B ratio can be improved by factor ~ 100 (JAM simulation)

Y. Higashi

Future prospects at GSI/FAIR

Proposed setup with FRS (FAIR phase-0)

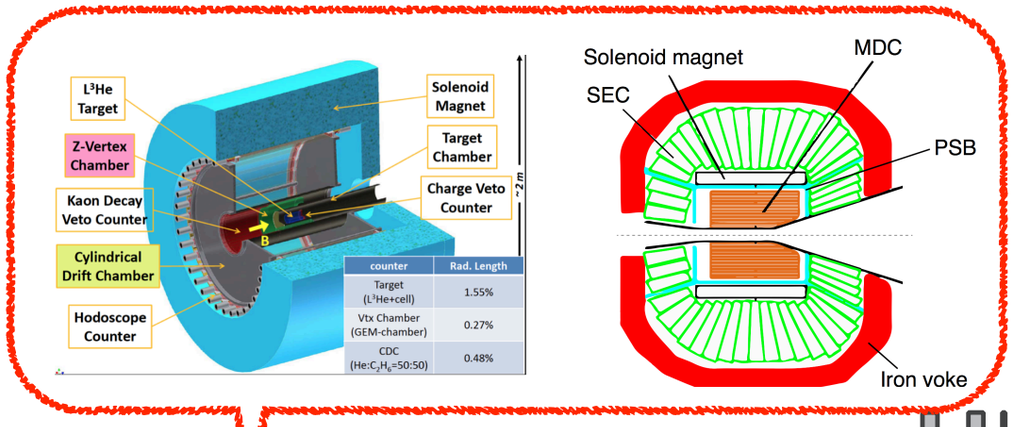

proton tagging w/ WASA-like ~4π detector

2.5 GeV proton from SIS-18

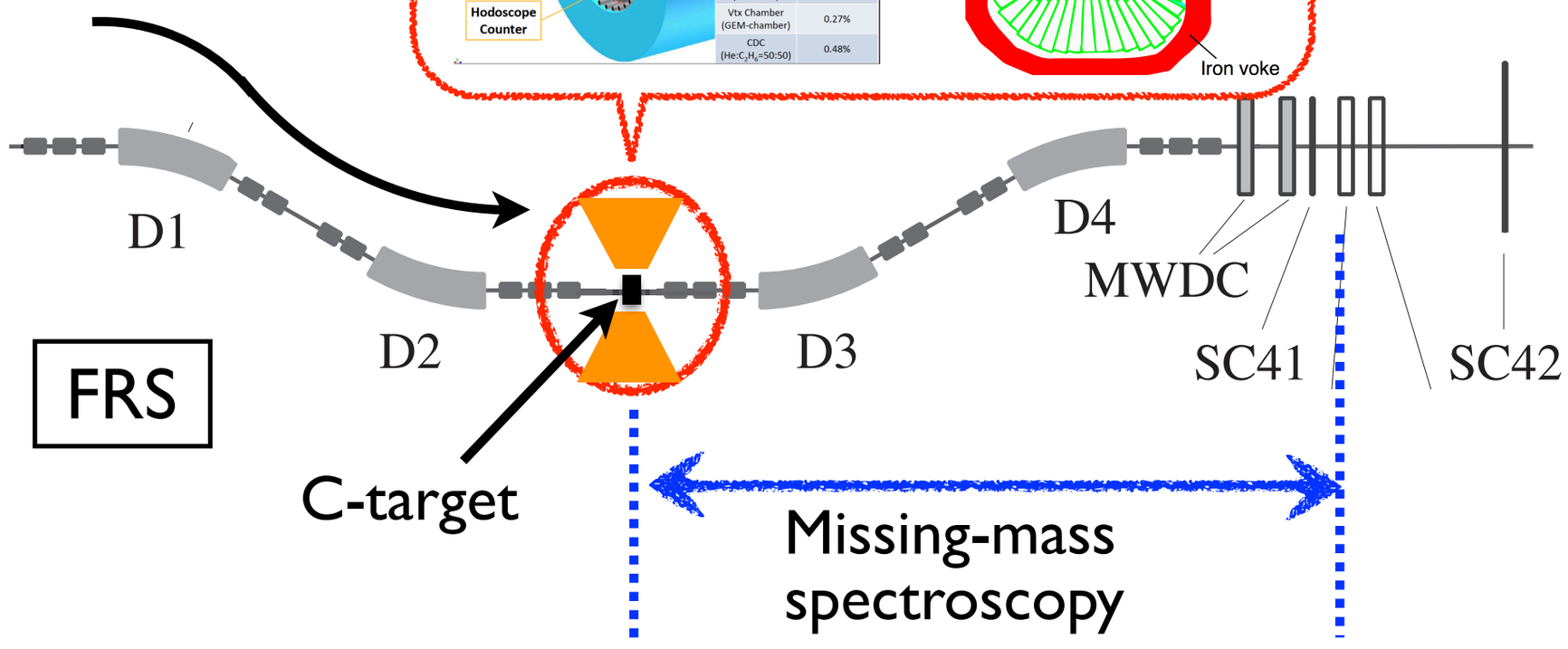

Versatile setup for high-resolution spectroscopy + decay tagging

- R&D for this experimental setup is ongoing.

Summary

◇ We have performed inclusive measurements of the ^{12}C(p,d) reaction aiming at the search for η′ mesic nuclei.

◇ Excitation-energy spectrum of ^{11}C near the η′ production threshold was successfully obtained with a high statistical sensitivity and sufficiently good resolution.

◇ Since no clear peak structure was observed, we determined upper limits for the formation cross sections of η′ mesic states.
Obtained limits around the η′ emission threshold are
$(d^2\sigma/d\Omega dE)_{95\%\text{C.L. limit}} \sim 20$ nb/(sr·MeV) at Γ = 5–15 MeV.

◇ Obtained spectrum has been compared with theoretically calculated spectra to discuss a constraint on η′-nucleus potential parameters (V_0, W_0).
$V_0 \sim -150$ MeV is excluded for $W_0 \lesssim 20$ MeV within this comparison.

◇ In order to improve experimental sensitivity, semi-exclusive measurement by tagging decay of η′ mesic nuclei is planned at GSI/FAIR.